Bachelor's Thesis

Bachelor's Degree in Industrial Technologies and Economic Analysis

Offshore Wind Park Optimization

June 2024

Author: Carles Roca Reverter

Supervisor: Josep Fanals i Batllori

Tutor: Oriol Gomis Bellmunt

Call: Spring 2023-2024

ETSEIB

Escola Tècnica Superior
d'Enginyeria Industrial de Barcelona

UPC

Abstract

Wind energy is one of the most promising renewable energy sources for the transition to a sustainable energy system. This thesis focuses on the study of the design and optimal sizing of a HVAC (High Voltage Alternating Current) transmission system for offshore wind power plants. It considers the possibility of incorporating reactive power compensation, including mid-cable, to reduce active power losses.

The work developed in this thesis includes the modelling of the electrical elements of an HVAC transmission system of an offshore wind power plant, the power flow analysis, the formulation of the optimization problem and the integration of a genetic algorithm to find a set of optimal solutions. The solver is integrated with Python and a specific case study is presented.

It is concluded that the proposed algorithm is applicable, meets the requirements imposed by the nature of the problem and that the use of a genetic algorithm is an efficient tool for finding optimal solutions.

Keywords: offshore wind power plant, power flow, renewable energy, HVAC, transmission system, optimization, genetic algorithms.

MSC codes: 90C11, 90C15, 90C29, 90C30, 90C59

ETSEIB

Resum

L'energia eòlica és una de les fonts d'energia renovable més prometedores per a la transició cap a un sistema energètic sostenible. Aquesta tesi se centra en l'estudi del disseny i dimensionament òptim d'un sistema de transmissió HVAC (High Voltage Alternating Current) per a parcs eòlics marins. Contempla la possibilitat d'incloure compensació de potència reactiva, incloent-hi a mig cable, per a reduir les pèrdues de potència activa.

El treball desenvolupat en aquesta tesi inclou el modelatge dels elements elèctrics d'un sistema de transmissió HVAC d'un parc eòlic marí, l'anàlisi del flux de potència, la formulació del problema d'optimització i la integració d'un algoritme genètic per a trobar un conjunt de solucions òptimes. El solucionador és integrat amb Python i es presenta un cas d'estudi específic.

Es conclou que l'algoritme proposat és aplicable, compleix els requisits imposats per la naturalesa del problema i que l'ús d'un l'algoritme genètic és una eina eficient per a trobar solucions òptimes.

Paraules clau: parc eòlic marí, flux de potència, energia renovable, HVAC, sistema de transmissió, optimització, algoritmes genètics.

Codis MSC: 90C11, 90C15, 90C29, 90C30, 90C59

ETSEIB

Resumen

La energía eólica es una de las fuentes de energía renovable más prometedoras para la transición hacia un sistema energético sostenible. Esta tesis se centra en el estudio del diseño y dimensionado óptimo de un sistema de transmisión HVAC (High Voltage Alternating Current) para parques eólicos marinos. Contempla la posibilidad de incluir compensación de potencia reactiva, incluyendo en medio cable, para reducir las pérdidas de potencia activa.

El trabajo desarrollado en esta tesis incluye el modelado de los elementos eléctricos de un sistema de transmisión HVAC de un parque eólico marino, el análisis del flujo de potencia, la formulación del problema de optimización y la integración de un algoritmo genético para encontrar un conjunto de soluciones óptimas. El solucionador es integrado con Python y se presenta un caso de estudio específico.

Se concluye que el algoritmo propuesto es aplicable, cumple los requisitos impuestos por la naturaleza del problema y que el uso de uno el algoritmo genético es una herramienta eficiente para encontrar soluciones óptimas.

Palabras clave: parque eólico marino, flujo de potencia, energía renovable, HVAC, sistema de transmisión, optimización, algoritmos genéticos.

Códigos MSC: 90C11, 90C15, 90C29, 90C30, 90C59

ETSEIB

Contents

Abbreviations and Symbols

The next list describes several abbreviations and symbols that will be later used within the body of the thesis.

Abbreviations

AC   Alternating Current

DC   Direct Current

GA   Genetic Algorithm

HVAC High Voltage Alternating Current

HVDC High Voltage Direct Current

N-R   Newton-Raphson Method

OPF   Optimal Power Flow

OSS   Offshore Substation

OWF   Offshore Wind Farm

OWPP Offshore Wind Power Plant

PF   Power Flow

SCR   Short Circuit Ratio

XLPE Cross-Linked Polyethylene

Symbols

$\mathbf{J}$ Jacobian matrix

$\mathbf{L}_i^x$ Inequality constraint limit

ω Angular frequency

θ Voltage angle

ETSEIB

$\underline{\theta}$ Characteristic angle

$\underline{Z_c}$ Characteristic impedance

B Susceptance

C Capacitance

c Penalty factor

G Conductance

I Complex current

i_o Open circuit current

I_{rated} Rated current of cables

L Inductance

n_{cables} Number of cables

P Active power

P_{Cu}^{loss} Cooper losses

P_{Fe}^{loss} Iron losses

p_{owf} Active power injection from the OWPP

Q Reactive power

q_{owf} Reactive power injection from the OWPP

R Resistance

S Complex power

S_n Rated power of cables

S_{r-tr} Rated power of the transformer

ETSEIB

u_k Short-circuit voltage

U_{r-tr} Rated voltage of the transformer at the transmission system side

V Complex voltage

V_{rated} Rated voltage of cables

Y Admittance

Z Impedance

List of Figures

ETSEIB

List of Tables

ETSEIB

1   Preface

The purpose of an Offshore Wind Power Plant (OWPP) is to capture and convert wind power energy into electrical energy and transmit it to the electrical grid. Therefore, a transmission system is needed to connect the OWPP to the grid.

Designing and sizing the transmission system is a non-trivial problem that has to be approached carefully. The goal is to minimize investment costs while ensuring the system to respect a set of technical constraints. Having insights on the tradeoff between these two different objectives is crucial to make informed decisions. To do so, a mathematical optimization problem can be formulated, allowing to find a set of optimal solutions that represent the relationship between the two objectives and at the same time respect the set of technical constraints. The power flow analysis is key to understand the steady-state behavior of the system and to formulate the optimization. Power flow equations are non-linear, and we need to solve them iteratively using numerical methods.

To put into context the relevance of this topic, the work and software developed in this thesis will be used as the breeding-ground of a partnership between eRoots and Acciona, a leading infrastructure company in Spain that has shown interest in developing a tool for the optimal design of OWPP's transmission systems.

All these concepts will be developed in this work and the reader should be able to understand the problem to its full extent through the reading of the thesis.

ETSEIB

2 Introduction

2.1 Motivation

During the industrial engineering studies you get in touch with a wide range of topics that can be applied to different fields. During the last years of your bachelor's degree you get introduced to electrical engineering fundamentals and its applications. I discovered a deep interests in those topics and realized is a key tool for ensuring a future towards energy systems that can integrate renewable energy sources. That is why I contacted Oriol Gomis to explore thesis topics within this field.

He introduced me to diverse research areas and also eRoots, a spin-off from the UPC-CITCEA that develops software solutions for modern grid modelling, analysis and optimization. Then Josep Fanals, my supervisor and eRoots CEO, presented various topics to me that I would be potentially interested to develop a thesis on. This is when he introduced me to the topic of design, sizing and optimization of the transmission system of OWPPs. The research group CITCEA-UPC has been working in this area [1] and further development on this field was the breeding ground for this proposal. The topic immediately caught my attention and that is how I ended up as an intern at eRoots developing software solutions for the optimization of OWPP.

The main driving force behind choosing this topic is the need to develop a sustainable energy system that can ensure a future for the next generations. The energy system is a key player in the fight against climate change. Moreover, the last report on global sustainable development [2] highlights how *Goal 7: Affordable and clean energy* is failing to meet its targets. In fact, it actually notices a backward trend in the 2020-2023 period when it comes to this goal targets, which signals that it is an area where efforts have to be put in.

This thesis is my modest and passionate contribution to provide sustainable solutions for our future.

2.2 Scope

This work will limit its study to :

- The optimal design of HVAC (High Voltage Alternating Current) transmission systems, without considering the comparison with HVDC (High Voltage Alternating Current).

- Study the steady-state of balanced three-phase load systems, without considering unbalanced or transient states.

- We will consider constant power injection from the OWPP at its nominal value. In this sense, we are not including the wind speeds distribution that yields different power injections.

- We will assume that the main grid we are supplying power to is completely stable, in the sense that it does not suffer voltage level perturbations.

ETSEIB

2.3   Objectives

The main objectives of the thesis are the following:

- Model all the elements of the transmission system of an offshore wind power plant and find its equivalent circuit.

- Implement a power flow solver with Python.

- Formulate the optimization problem of the reactive power compensation and the transmission system design.

- Design and implement an optimization algorithm in Python that allows to find the Pareto Frontier of optimal solutions and compare its advantages with respect to the state-of-the-art.

- Study a specific case study applicable to real offshore wind power plants.

2.4   Outline

The thesis is structured as follows:

- Chapter 3 introduces offshore wind power plants, the problem we want to tackle and models the elements that we find in a HVAC transmission system.

- Chapter 4 presents the power flow analysis and builds the full transmission system model.

- Chapter 5 formulates the minimization problem, including objective functions and constraints. In this section we describe the algorithm structure that deals with the optimization formulation.

- Chapter 6 explains state-of-the-art methods to solve the problem, its limitations, and our new approaches, involving genetic algorithms and an optimal power flow method.

- Chapter 7 showcases the results for a specific case study and analyses the performance and results of the optimization algorithm.

- Chapter 8 collects the main outcomes of the thesis and proposes future lines of work.

- Chapter 9 presents the planning and viability studies for the project.

ETSEIB

3 Technical Background and Modelling

3.1 Offshore Wind Power Plant

As global energy demands surges and the pressing need for sustainable development becomes ever more urgent, the quest for renewable energy sources has intensified. Among these, wind power has emerged as a front-runner due to its potential to generate substantial amounts of clean electricity. While onshore wind farms have been widely implemented, their offshore counterparts are gaining increasing attention for their ability to harness the stronger and more consistent winds found over the oceans.

Offshore wind power, defined as the use of wind turbines located in bodies of water to generate electricity, presents several advantages over onshore installations. The primary benefit lies in the higher wind speeds and lower turbulence experienced offshore, which contribute to greater energy yields. Additionally, offshore wind farms can be situated closer to urban centers located along coastlines, thereby reducing transmission losses and enhancing energy efficiency. The development of offshore wind technology has seen rapid advancements in recent years. From the deployment of the first offshore wind farm in Denmark in 1991 to the establishment of massive installations such as the Hornsea Project in the UK [3], the scale and capacity of these projects have grown significantly. Technological innovations, including larger turbines, floating foundations, and improved grid integration techniques, have further propelled the industry forward.

3.2 Transmission System: Design and Reactive Power Compensation

When designing the transmission system of an OWPP, several factors must be considered to ensure optimal performance and efficiency. The system must be capable of transmitting the generated power from the wind turbines to the onshore grid while trying to be as energy and cost-efficient as possible. There are two main types of technologies that can be used, HVDC and HVAC. In this thesis we will focus our study to the HVAC technology.

One drawback of using HVAC cables is the high shunt capacitance they have, which is even larger in underground cables, which are the ones used for OWPP.

	Overhead Lines	Underground Lines
Capacitance per unit length (μF/km)	0.01 - 0.02	0.3 - 0.6

Table 1: Comparison of Capacitance per unit length of overhead and underground Lines, [4] and [5].

The charging current of this capacitance limits the active power transfer capacity of the line and increases power losses and voltage across the line due to the Ferranti effect [6]. This effect can be described by the voltage difference between the sending and receiving end of transmission line under no-load conditions:

$$\frac{V_o - V_i}{V_o} = \omega^2 C L \frac{l^2}{2} \tag{1}$$

ETSEIB

where V_o and V_i are the receiving and sending end voltages respectively, ω is the frequency, C is the capacitance per unit length, L is the inductance per unit length and l is the length of the line. Note that the voltage difference is proportional to the square of the length of the line which leads to overvoltages for long transmission lines.

However, the possibility to include reactive power compensation elements helps reduce the reactive power generation. Fig. 1 shows how including this compensation reduces power losses, especially when we approach the no-load condition, which is equivalent to not having any type of active power injection from the OWPP, i.e. the wind speed is very low.
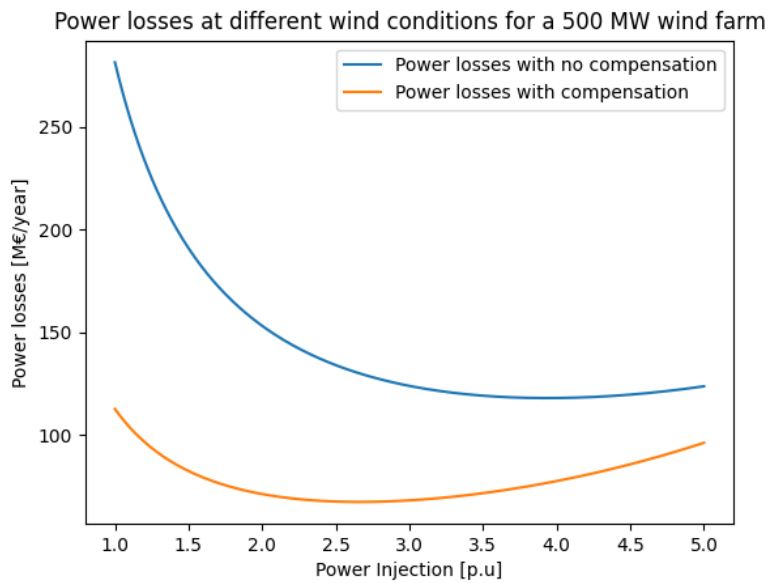
Figure 1: Power losses comparison when including mid-cable reactive power compensation.

The goal of the project is to determine where this compensation has to be placed and how to size it. But this is only part of the design characteristics we want to optimize. A full description of the optimization variables will be presented in Chapter 5.

Taking all this into consideration, a HVAC transmission system layout for an OWPP with reactive power compensation looks like the one in Fig. 2.
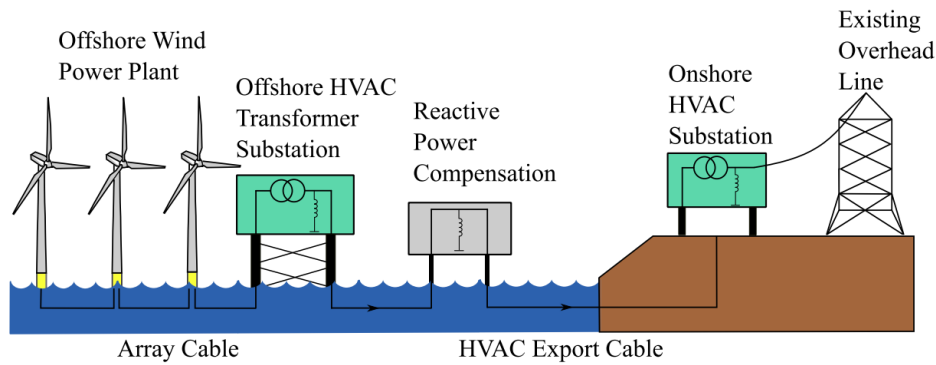
Figure 2: HVAC transmission system layout for an OWPP with reactive power compensation [1].

From this general layout we will be able to create the network model using the equivalent circuits of the elements involved.

3.3 Elements Modelling

To be able to do a steady-state analysis of the transmission system we need to model all the elements in the grid. This section models these elements and presents some important concepts to understand the system.

3.3.1 Cables

Cables are an essential part of HVAC transmission systems, since they are in charge of transmitting the power from the OWPP to shore and are the main source of active power losses and reactive power generation. We will consider three-core cross-linked Polyethylene (XLPE) cables, which are the most common type of cables used in AC OWPP's since they are specifically designed for underwater applications, and they have lower dielectric losses than EPR (Ethylene Propylene Rubber) or fluid-filled cables [7].

Three-core XPLE cables (see Fig. 3) have a steel wire armour and can have either copper or aluminum as conductor. We will consider the cooper ones since they have higher current rating at the same cross-section [4].

Figure 3: Three-core XLPE cable cross-section [4].

Recall, as seen in 1, that the capacitance of underground cables is quite large, which leads to high reactive power generation. Reactive power compensation will help us mitigate this effect.

For the equivalent circuit of a long transmission cables, we can use the following π-model, shown in Fig. 4.
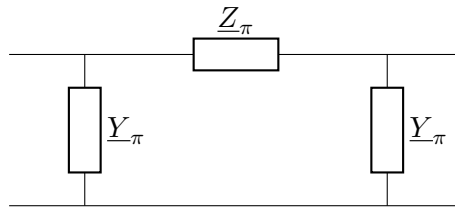
Figure 4: π-model transmission line.

We can use the following equations [1] to get the parameters:

$$\begin{bmatrix} \underline{V}_s \\ \underline{I}_s \end{bmatrix} = \begin{bmatrix} \cosh(\underline{\theta}) & \underline{Z}_c \sinh(\underline{\theta}) \\ \frac{1}{\underline{Z}_c} \sinh(\underline{\theta}) & \cosh(\underline{\theta}) \end{bmatrix} \begin{bmatrix} \underline{V}_r \\ \underline{I}_r \end{bmatrix} \tag{2}$$

$$\underline{Z}_c = \sqrt{\frac{\underline{Z}}{\underline{Y}}}; \quad \underline{\theta} = l\sqrt{\underline{Z}\underline{Y}} \tag{3}$$

$$\underline{Z} = R + j\omega L; \quad \underline{Y} = j\omega\frac{C}{2} \tag{4}$$

where $\underline{V}_s$ and $\underline{I}_s$ are the sending end voltage and current and $\underline{V}_r$ and $\underline{I}_r$ are the receiving end voltage and current, $\underline{Z}_c$ is the characteristic impedance and $\underline{\theta}$ is the characteristic angle. The parameters in Table 2 are obtained from manufacturer data [4].

ETSEIB

Symbol		Description
R	$\left[\frac{\Omega}{\text{km}}\right]$	Resistance per unit length
L	$\left[\frac{H}{\text{km}}\right]$	Inductance per unit length
C	$\left[\frac{F}{\text{km}}\right]$	Capacitance per unit length

Table 2: Electrical parameters of AC cables.

Therefore, the equivalent π model is given by:

$$\underline{Z}_\pi = \underline{Z}_c \sinh(\underline{\theta}) = \underline{Z}l \frac{\sinh(\underline{\theta})}{\underline{\theta}} \tag{5}$$

$$\underline{Y}_\pi = \frac{\tanh(\underline{\theta}/2)}{\underline{Z}_c} = \frac{\underline{Y}l}{2} \frac{\tanh(\underline{\theta}/2)}{\underline{\theta}/2} \tag{6}$$

3.3.2   Transformers

Transformers are essential devices in power transmission systems that transfer electrical energy between circuits through electromagnetic induction. They enable voltage levels to be increased (stepped up) for efficient, long-distance transmission and decreased (stepped down) for safe distribution to homes and businesses. This voltage transformation minimizes energy losses and enhances the stability of the power grid. Without transformers, the high currents required for low-voltage transmission would lead to excessive heat generation and energy losses, reducing the efficiency and reliability of the electrical supply. Thus, transformers are crucial for optimizing power delivery and ensuring the safety and efficiency of electrical systems.

In our OWPP transmission system we will need to employ transformers to step up the voltage of the power generated by the wind turbines to the nominal voltage of the transmission system and another one at onshore to set the voltage required by the main grid we are supplying to.

We will use the model in Fig. 5 to represent the transformer:
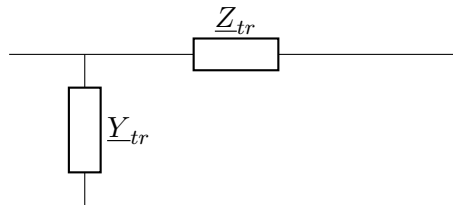
Figure 5: Transformer model.

ETSEIB

The equivalent impedance $\underline{Z}_{tr}$ and admittance $\underline{Y}_{tr}$ are given by [1]:

$$\underline{Z}_{tr} = R_{tr} + jX_{tr}; \quad \underline{Y}_{tr} = G_{tr} + jB_{tr} \tag{7a}$$

$$R_{tr} = P_{Cu}^{loss}\left(\frac{U_{r-tr}}{S_{r-tr}}\right)^2 \quad X_{tr} = \sqrt{\left(u_k\frac{U_{r-tr}}{S_{r-tr}}\right)^2 - R_{tr}^2} \tag{7b}$$

$$G_{tr} = \frac{P_{Fe}^{loss}}{U_{r-tr}^2} \quad B_{tr} = i_o\frac{S_{r-tr}}{U_{r-tr}^2} \tag{7c}$$

where P_{Cu}^{loss} are the copper losses, U_{r-tr} the rated voltage of the transformer at the transmission system side, S_{r-tr} the rated power of the transformer, u_k the short-circuit voltage, P_{Fe}^{loss} the iron losses and i_o the open circuit current.

3.3.3   Shunt Reactors: Reactive Power Compensation

To compensate reactive power generation we will use shunt reactors. They are reactive power absorbers and in our case will be connected from the line directly to the ground. The equivalent circuit is shown in Fig. 6.

$$\underline{y}_{sh} = \frac{1}{j\omega L} \tag{8}$$

where L is the inductance of the reactor.
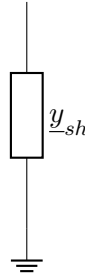
Figure 6: Shunt reactor model.

We will consider the possibility to include 5 different shunt reactors in the system. Further development on the reasoning of this scheme on Chapter 4.

3.3.4   Main Grid

The main grid is the distribution grid we are supplying power to fit the OWPP. We will model the grid we are connected to using a Thévenin equivalent circuit where $\underline{U}_g$ is the Thévenin voltage and $\underline{Z}_g$ is the Thévenin impedance [1]:
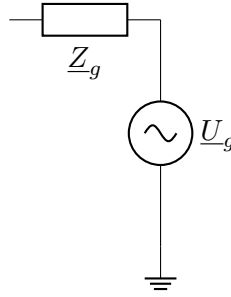
Figure 7: Main grid model.

The equations describing the Thévenin equivalent circuit are:

$$\underline{Z}_g = R_g + jX_g \tag{9a}$$

$$R_g = \sqrt{\frac{\frac{U_g^2}{SCR} p_{owf} S_{base}}{(\frac{X_g}{R_g})^2 + 1}} \tag{9b}$$

$$X_g = R_g \frac{X_g}{R_g} \tag{9c}$$

where U_g is the rated voltage of the grid, SCR the short-circuit ratio and $\frac{X_g}{R_g}$ the ratio of the system reactance.

- The SCR is the ratio of the short circuit apparent power in the case of a balanced fault at the location in the grid where some generator is connected to the power rating of the generator itself. It is somehow a measure of the grid strength to changes in active and reactive power injections.

3.3.5   Offshore Wind Power Plant

We will model our OWPP as a simple power injection at one end of the transmission line. For our analysis we will consider that there is no reactive power generation, therefore $q_{owf} = 0$. p_{owf} will be the active power generation that will depend on the wind conditions of the plant. The reach of the work will limit its analysis to a fix power generation.
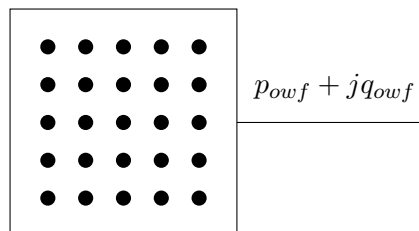
Figure 8: Offshore Wind Power Plant.

Further development on how considering different wind conditions could be implemented in our work, check section 8.2.

3.4   Costs Modelling

In this section we will derive the cost equations for the different elements of our transmission system. These costs function will be essential for our optimization problem since they will be the objective function to minimize and the parameters on which the vector of decision variables we want to get will depend on.

3.4.1   Cables

Equations to describe AC cables costs are presented in [12] as:

$$C_{cables} = n_{cables}(A + B\exp(\frac{CS_n}{10^8})) \cdot E_{\frac{eu}{sek}} \cdot \frac{1}{10^6} \quad \left[\frac{M\mathord{\text{\euro}}}{\text{km}}\right] \tag{10}$$

$$S_n = \sqrt{3}V_{rated}I_{rated} \quad [\text{VA}] \tag{11}$$

where S_n is the rated power of the cable, n_{cables} is the number of cables, A, B and C are parameters that depend on the rated voltage of the cable, $E_{\frac{eu}{sek}=0.087}$ is the exchange rate between Euros and SEK (Swedish Króna) and V_{rated} and I_{rated} are the rated voltage and current of the cable respectively. The parameters A, B and C are shown in Table 3:

Rated Voltage (kV)	A $[10^6]$	B $[10^6]$	C
132	1.971	0.209	1.66
220	3.181	0.11	1.16

Table 3: Parameters A, B, C for different rated voltages [12].

We will consider the transmission voltage levels presented in Table 3 as decision variables in our optimization.

3.4.2   Transformers

For the transformers, costs are defined in [23] as:

$$C_{tr} = 0.0427 \cdot S_{r-tr}^{0.7513} \quad [M\mathord{\text{\euro}}] \tag{12}$$

where S_{r-tr} is the rated power of the transformer in MVA.

3.4.3   Shunt Reactors

Cost functions for shunt reactors are presented in [1] as:

$$C_{sh} = K \cdot Q_l \cdot +P = K \cdot Y_l \cdot U_{AC-N}^2 + P \quad [M\mathord{\text{\euro}}] \tag{13}$$

where K and P are constants that depends on the location of the reactor and can be found in Fig. 4,

ETSEIB

$Q_l = Y_l \cdot U_{AC-N}^2$ is the reactive power absorbed by the reactor in MVAr, Y_l is the admittance of the reactor and U_{AC-N} is the nominal transmission voltage where the compensation is placed.

Location	K	P
Onshore	0.01049	0.8312
Offshore	0.01576	1.244
Mid-cable	0.01576	12.44

Table 4: Parameters K and P for different positions of the reactive power compensation [1].

3.4.4 Switchgears

For switchears, costs are defined in [13] as:

$$C_{gis-AC} = 0.0117 \cdot U_{AC-N} + 0.0231 \quad [M€] \tag{14}$$

where U_{AC-N} is the nominal transmission voltage in kV.

3.4.5 Substation Platform

For the substation platform, costs are presented in [12] as:

$$C_{ss-AC} = 2.534 + 0.0887 \cdot P_{owf} \quad [M€] \tag{15}$$

where P_{owf} is the nominal power generated by the OWPP in MW.

3.4.6 AC Power Losses

Lastly, but probably one of the most important costs to consider, are the power losses in the transmission system. To be able to compare this term with other investment costs related to the electric elements, it would be useful to express this term in monetary units. We will use the following equation to estimate the cost of power losses in the system:

$$C_{loss-AC} = 8760 \cdot t_{owf} \cdot C_{energy} \cdot P_{loss} \cdot 10^{-6} \quad [M€] \tag{16}$$

where 8760 is the number of operating hours in a year, t_{owf} is the expected lifetime of the OWPP in years, C_{energy} is the cost of energy in €/MWh and P_{loss} is the power losses in the system in MW. We will be using the following estimated values from [1]:

Parameter	Value
t_{owf}	30 years
C_{energy}	100 €/MWh

Table 5: Parameters for computing power losses cost [1].

ETSEIB

Now it remains to compute the power losses P_{losses} in the system. This will be derived in section 4 as it will be trivial to get the power losses once we have the power flow solution.

4 Power Flow Analysis

Now we can fully define the power flow analysis. This approach will allow as to model the transmission system as a set of buses (or nodes) interconnected by transmission links. It will allow as to solve for the steady-state powers and voltages of the system. This step is crucial to latter on formulate our optimization since power flow equations will be the equality constraint of the optimization problem, see section 5.1.1, and the objective function will also depend on the solution of the power flow (PF).

4.1 Types of Buses

In this section we will briefly describe what is a bus and what types we have.

Buses are points of the grid which either supplied by generators, *generator buses*, or those without generators, *load buses*. More formally, an n-bus system, $N = \{B_1, ..., B_i, ..., B_n\}$ where N is the set of n-nodes, is defined as:

$$\forall B_i \in N, \begin{cases} S_i = P_i + jQ_i, & \text{where } S_i \text{ is the apparent power at bus } i \\ V_i = |V_i|e^{j\theta_i}, & \text{where } V_i \text{ is the complex voltage at bus } i \end{cases} \tag{17}$$

As we can see, for each bus i we have 4 variables:

- P_i and Q_i are the active and reactive power at bus i respectively.

- $|V_i|$ and θ_i are the voltage magnitude and angle at bus i respectively.

It is important to note that in general we cannot specify all the P_i's independently since there is a constraint imposed by the need to balance active power. In our case, a transmission system with losses, which are unknown before the PF, the sum of P_i's must be equal to losses. To tackle this we will define one bus as the *slack* bus, where power injection is left free. Taking all of this account, depending on the variables are known and unknown for a certain bus we can classify them as:

- **Slack bus:** The slack bus is the reference bus of the system. It is the bus where the voltage magnitude and angle are known, typically $|V_i| = 1, \theta_i = 0$. All other buses angles will be referenced to the *slack*. It is used to balance the active and reactive power in the system.

- **Generator bus (PV):** The generator bus is the bus where the active power and voltage are known.

- **Load bus (PQ):** The load bus is the bus where the active and reactive power are known. The voltage magnitude and angle are unknown.

In summary:

	Slack Bus	PQ	PV
Voltage Magnitude ($|V_i|$)	Yes	No	Yes
Voltage Angle (θ_i)	Yes	No	No
Active Power (P_i)	No	Yes	Yes
Reactive Power (Q_i)	No	Yes	No

Table 6: Known variables for each type of bus.

4.2 Per-Unit System (p.u.)

In power systems analysis, it is common to use the per-unit system to normalize the magnitudes of the variables. This is very useful when we are dealing with several transformers and voltage levels. The per-unit system is defined as:

$$\text{Per unit value} = \frac{\text{Actual value}}{\text{Base value}} \tag{18}$$

In our case we will use $S_{base} = 100$ MVA and $V_{base} = $ transmission voltage in kV as the base values. This means that the per-unit system will be defined as:

$$\begin{cases} I_{base} = S_{base}V_{base} \\ Y_{base} = \frac{S_{base}}{V_{base}^2} \end{cases} \tag{19}$$

Using the per-unit system will be particularly useful for analyzing the results and for dealing with the inequality constraints in section 5.1.2.

4.3 Full Transmission System Model

Now we have all the information needed to build our full model. In [1] they consider five possible positions for the shunt reactors, as seen in Fig. 9.

Figure 9: Possible locations for the shunt reactors [1].
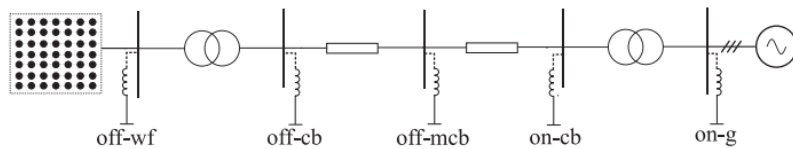
They consider when optimizing the cost function only the combinations where: if at a given transformer you place a reactor before it, you won't consider placing another one after the same transformer. For sake of generality, we will consider that any combination within the five possible positions is valid. This will lead to a total of $2^5 = 32$ possible combinations.
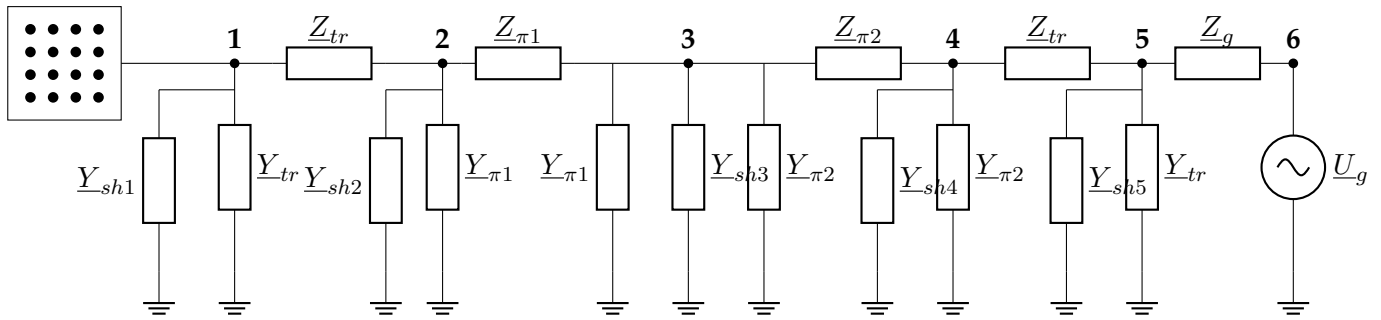
Figure 10: Transmission system model and buses.

Now we choose where we want to define our buses and which type they are. We classify them as in Table 7.

Bus Number	Bus Type
1	PQ
2	PQ
3	PQ
4	PQ
5	PQ
6	Slack

Table 7: Transmission system bus types.

A brief explanation of the bus types is exposed:

- **Bus 1:** It is the bus where the OWPP is injecting power therefore active and reactive power are specified as $P_1 = p_{owf}$ and $Q_1 = q_{owf}$.

- **Bus 2, 3, 4, 5:** Those buses are plain PQ load buses, where $P_i = 0, Q_i = 0$. We want to consider them as we will be interested in the voltage levels in the lines in order to compute possible over and undervoltages in the cables, as we will see in Chapter 5.

- **Bus 6:** We will use this one as the slack bus. Note that this bus power flow solution for P_6 will allow us to compute the losses in the system and will be essential part of the optimization problem. Also, since we define it as the slack bus, it will be the reference for the voltage angles and in charge of balancing the power in the transmission system.

4.4 Admittance Matrix

The admittance matrix encodes all the information of the passive elements of the grid and the relationship between them and allows us to perform the steady-state analysis of the grid. Now we can build the full HVAC transmission system model and fins its admittance matrix $\underline{Y}_{bus}$, which will be essential for the power flow solver.

Inspecting the Kirchhoff's Current Law (KCL) we can observe how the admittance matrix is the fundamental relationship between voltages and currents :

$$\mathbf{I} = \mathbf{Y}_{bus}\mathbf{V} \tag{20}$$

where $\mathbf{I}$ is the vector of injected currents, $\mathbf{Y}_{bus}$ is the admittance matrix and $\mathbf{V}$ is the vector of bus voltages.

Since we will be using the per-unit system:

$$y_i = \frac{Y_i}{Y_{base}} \tag{21}$$

Note that when we build $\mathbf{Y}_{bus}$, we take the series impedance in Eq. 10, compute their inverse and add the sub-index s to identify them. For example:

$$\underline{y}_{\pi 1s} = \frac{1}{\underline{z}_{\pi 1}} \tag{22}$$

$$\mathbf{Y_{bus}} = \begin{bmatrix} (\underline{y}_{tr} + \underline{y}_{trs} + \underline{y}_{sh1}) & -\underline{y}_{trs} & 0 & 0 & 0 & 0 \\ -\underline{y}_{trs} & (\underline{y}_{\pi 1} + \underline{y}_{\pi 1s} + \underline{y}_{sh2} + \underline{y}_{trs}) & -\underline{y}_{\pi 1s} & 0 & 0 & 0 \\ 0 & -\underline{y}_{\pi 1s} & (2\underline{y}_{\pi 1} + 2\underline{y}_{\pi 1s} + \underline{y}_{sh3}) & -\underline{y}_{\pi 2s} & 0 & 0 \\ 0 & 0 & -\underline{y}_{\pi 2s} & (\underline{y}_{\pi 2} + \underline{y}_{\pi 2s} + \underline{y}_{sh4} + \underline{y}_{trs}) & -\underline{y}_{trs} & 0 \\ 0 & 0 & 0 & -\underline{y}_{trs} & (\underline{y}_{tr} + \underline{y}_{tr} + \underline{y}_{sh5} + \underline{y}_{g}) & -\underline{y}_{g} \\ 0 & 0 & 0 & 0 & -\underline{y}_{g} & \underline{y}_{g} \end{bmatrix} \tag{23}$$

Some properties of the admittance matrix are:

- It is a square matrix of size $n \times n$, where n is the number of buses in the system.

- It is symmetric. Note that this condition does not hold for certain types of transformers.

- The diagonal elements, Y_{ii}, are self-admittance, equal to the sum of the admittances of elements connected to bus i. Note that this condition does not hold for certain types of transformers.

- Y_{ij} is the negative of the admittance between buses i and j.

- For our system, the sparcity is $\frac{20}{36} = 56\%$. Nevertheless, for large networks, the matrix is very sparse. The level of sparsity, which is the percentage of zero elements in a matrix, increases with the size of the network. For instance, in a 1000-bus system, the matrix approximately is 99% sparse. You can take advantage (and it will be essential to do it for very big networks) of this sparsity using computational techniques [9].

ETSEIB

4.5   Transmission System Parameters

We will use the following set of grid elements parameters for the transformers and the main grid:

Parameter	Value
SCR	5
$\frac{X_g}{R_g}$	10
P_{Cu}^{loss}	60 kW
P_{Fe}^{loss}	40 kW
u_k	18 %
i_o	1.2 %

Table 8: Grid parameters [1].

4.6   Power Flow

4.6.1   Power Flow Equations

We are first going to derive an expression for the PF equations. From Eq. 20 we can get the injected current for the i-th component:

$$I_i = \sum_{j=1}^{n} Y_{ik} V_k \quad i = 1, 2, ..., n \tag{24}$$

Now we can compute the i-th bus power:

$$S_i = V_i I_i^* = V_i \sum_{k=1}^{n} Y_{ik}^* V_k^* \quad i = 1, 2, ..., n \tag{25}$$

Now if we let $V_i = |V_i| e^{j\theta_i}$, and $Y_{ik} = G_{ik} + jB_{ik}$, we can write the power at bus i as:

$$S_i = \sum_{k=1}^{n} |V_i||V_k| e^{j\theta_i} (G_{ik} - jB_{ik}) = \sum_{k=1}^{n} |V_i||V_k| (cos(\theta_{ik}) + jsin(\theta_{ik}))(G_{ik} - jB_{ik}) \quad i = 1, 2, ..., n \tag{26}$$

Note that the real part of the admittance, G_{ik}, is the conductance and the imaginary part, B_{ik}, is the susceptance. Now if we separate the real and imaginary parts of the power we get:

$$P_i = \sum_{k=1}^{n} |V_i||V_k| (G_{ik} cos(\theta_{ik}) + B_{ik} sin(\theta_{ik})) \quad i = 1, 2, ..., n \tag{27}$$

$$Q_i = \sum_{k=1}^{n} |V_i||V_k| (G_{ik} sin(\theta_{ik}) - B_{ik} cos(\theta_{ik})) \quad i = 1, 2, ..., n \tag{28}$$

4.6.2   Newton-Raphson Solver

Problem Solvability   First, we have to make sure that our set of equations is solvable. If we strip away the $slack$-bus, we have 5 PQ-buses remaining. Each PQ-bus introduces 2 unknowns, $|V_i|$ and θ_i, and 2 equations, P_i and Q_i. This means that we have 10 equations and 10 unknowns. After solving the system, from Eq. 27 and Eq. 28 we can solve for the power injections of the slack bus, P_6 and Q_6. Hence, the condition for solvability is fulfilled.

To solve a set of non-linear equations, numerical methods are the standalone way to go. For the PF, one of the most used methods is the Newton-Raphson (N-R) method [10]. A brief description of this method will be presented for the n-dimentional case, but further description can be found in [8].

We will describe the process considering an n-bus system with all PQ buses except one slack bus. Note that in our specific case these conditions are met and $n = 6$. Once we strip away the slack bus, it remains to find the unknowns on the right side of Eqs. 27 and 28. Therefore, it will be convenient to define the following vectors of unknowns of PQ-buses:

$$
\theta = \begin{bmatrix} \theta_1 \\ \theta_2 \\ \vdots \\ \theta_{n-1} \end{bmatrix} \quad |\mathbf{V}| = \begin{bmatrix} |V_1| \\ |V_2| \\ \vdots \\ |V_{n-1}| \end{bmatrix} \quad \mathbf{x} = \begin{bmatrix} \theta \\ |\mathbf{V}| \end{bmatrix} \tag{29}
$$

Now the dependency between the power flow equations and the vector of unknowns $\mathbf{x}$ can be easily shown:

$$
P_i = P_i(\mathbf{x}) \quad i = 1, 2, ..., n-1 \tag{30a}
$$

$$
Q_i = Q_i(\mathbf{x}) \quad i = 1, 2, ..., n-1 \tag{30b}
$$

The N-R method is an iterative method that starts with an initial guess of the unknowns, $\mathbf{x}_0$, and then iterates the vector $\mathbf{x}$ until the right side matches the left side of the equations. Therefore, we can define the power mismatch vector $\mathbf{f}(\mathbf{x})$ as:

$$
\mathbf{f}(\mathbf{x}) = \begin{bmatrix} P_1(\mathbf{x}) - P_1 \\ \vdots \\ P_{n-1}(\mathbf{x}) - P_{n-1} \\ Q_1(\mathbf{x}) - Q_1 \\ \vdots \\ Q_{n-1}(\mathbf{x}) - Q_{n-1} \end{bmatrix} = \begin{bmatrix} \mathbf{\Delta P(x)} \\ \mathbf{\Delta Q(x)} \end{bmatrix} = \mathbf{0} \tag{31}
$$

ETSEIB

Now we have to consider $\mathbf{J}$, the Jacobian matrix of $\mathbf{f}(\mathbf{x})$. For clarity, is convenient to partition $\mathbf{J}$ as:

$$\mathbf{J} = \begin{bmatrix} \mathbf{J_{11}} & \mathbf{J_{12}} \\ \mathbf{J_{21}} & \mathbf{J_{22}} \end{bmatrix} = \begin{bmatrix} \frac{\partial \mathbf{\Delta P}}{\partial \theta} & \frac{\partial \mathbf{\Delta P}}{\partial |\mathbf{V}|} \\ \frac{\partial \mathbf{\Delta Q}}{\partial \theta} & \frac{\partial \mathbf{\Delta Q}}{\partial |\mathbf{V}|} \end{bmatrix} = \begin{bmatrix} \frac{\partial \mathbf{P}}{\partial \theta} & \frac{\partial \mathbf{P}}{\partial |\mathbf{V}|} \\ \frac{\partial \mathbf{Q}}{\partial \theta} & \frac{\partial \mathbf{Q}}{\partial |\mathbf{V}|} \end{bmatrix} \tag{32}$$

If interested, check derivation of the partial derivatives of the power flow equations with respect to the unknowns check the Appendix or [8].

Now it just remains to find the step $\Delta \mathbf{x^k}$ to update $\mathbf{x}$ solving the following linear system by Gauss elimination:

$$\mathbf{J^k} \Delta \mathbf{x^k} = -\mathbf{f}(\mathbf{x^k}) \tag{33}$$

Now we update $\mathbf{x^{k+1}} = \mathbf{x^k} + \Delta \mathbf{x^k}$ and iterate until it converges. The convergence criteria will be usually set as the maximum of the absolute value of the power mismatch vector, $\max(\mathbf{f}(\mathbf{x}))$, is less than a tolerance, tol, which we have set to 10^{-6}.

The N-R solver has been implemented in Python(check the Appendix) and the procedure can be found in Algorithm 1.

Algorithm 1 Newton-Raphson Method

---

procedure RUN_PF
    Initialize V with ones and θ with zeros
    Set $V[slack]$ to 1, $\theta[slack]$ to 0
    Set P, Q based on OWPP data
    Set $iter = 0$, tol and $k = 0$
    while $iter < max\_iter$ and $\Delta PQ > tol$ **do**
        Compute $P\_present$, $Q\_present$ using V, θ, Y_{bus}
        Compute mismatch $\Delta PQ = [dP, dQ]$ as difference between calculated and given P, Q
        Compute the Jacobian matrix J.
        Solve the linear system $J \cdot \Delta x_k = -\Delta PQ$.
        Compute the updated $x^{k+1} = x^k + \Delta x^k$.
        Update V, θ using dP, dQ, Y_bus
        if $\max(\Delta PQ) < tol$ **then**
            break
        end if
    end while
    return V, θ
    Compute P_{slack}, Q_{slack}
end procedure

Finally, note that close to the solution vector $\mathbf{x}^*$ it can be proven that N-R normally presents quadratic convergence [11]. Moreover, in terms of computational time, Algorithm 1 takes about $0.06\,\mathrm{s}$ in average to solve the PF.

ETSEIB

Now we can observe that the PF is essential for computing the power losses (see Eq. 16) in the system, which will be in the objective function of the optimization problem. It is clear to see that P_{losses} will be the difference between the injected active power from the OWPP and the active power delivered to the slack bus, which is the main grid:

$$P_{losses} = (P_{owf} - P_6) \cdot S_{base} \cdot 10^{-6} \quad \text{MW} \tag{34}$$

5   Optimization Problem Formulation

Generally an optimization problem that involves equality and inequality constraints can be formulated as:

$$\begin{aligned} \min \quad & \mathbf{f}(\mathbf{x}) = (f_1(x), f_2(x), ...,, f_k(x)) \\ \text{subject to} \quad & \mathbf{H}(\mathbf{x}) = 0 \\ & \mathbf{G}(\mathbf{x}) \le 0 \end{aligned} \qquad (35)$$

where $\mathbf{x} \in \mathbb{R}^n$ is the n decision variables vector, $\mathbf{f}(\mathbf{x}) \in \mathbb{R}^k$ is set of objective functions to be minimized. Note we have presented the problem in its more general form, where the objective function can be a set of n-objectives to have to be optimized simultaneously and will be proved to be useful in section 5.2. $\mathbf{H}(\mathbf{x}) = \mathbf{0}$ are the equality constraints and $\mathbf{G}(\mathbf{x}) \le \mathbf{0}$ are the inequality constraints.

Now we have to decide which decision variables we include in the optimization problem. It is easy to see that we can include all the design variables in which the transmission system model depends, which are all included in the cost function and therefore have a direct impact in the cost of the system. By checking the parameters on which the admittance matrix depends, which can be found in section 3, we can define the vector of unknowns as:

$$\mathbf{x} = \begin{bmatrix} vol_{tr}, & n_{cables}, & react_{bi_1}, & ,... & ,react_{bi5} & ,react_{cont1} & ,... & ,react_{cont5} & ,react_{bi5} & ,S_{trafo} \end{bmatrix} \qquad (36)$$

where the size of $\mathbf{x}$ is (1×13), i.e. we have 13 decision variables. Each term is defined as follows:

- vol_{tr}: Is the voltage level of the transmission cables. Note that this will be an integer variable, where you can choose one voltage level given by manufacturers with its associated parameters and cost. Check Table 3 to see available options considered.

- n_{cables}: Is an integer number that that represents the number of cables placed in parallel.

- $react_{bi_i} \quad i = 1, ..., 5$: Is a binary variable (i.e. either 0 or 1) that tells if we place or not a reactor at position i.

- $react_{cont_i} \quad i = 1, ..., 5$: Sizing of reactor at position i, therefore its Y_{shi} in p.u.

- S_{trafo}: Rated power of the transformer in VA.

A very important remark with respect to the type of variables we have involved in the problem. Considering $\mathbf{x}$ we see that we have binary, integer and continuous variables. This kind of problems are labeled as mixed-variable optimization and constraints the optimization methods we can use as we will see in 6.

5.1   Constraints

5.1.1   Equality: Power Flow

The equality constraints $\mathbf{H}(\mathbf{x}) = 0$ in the optimization problem in Eq. 35 are the imposed by the power flow equations. In fact, the power mismatch vector in Eq. 31 is the one that take this form. Therefore:

$$\mathbf{H}(\mathbf{x}) = \begin{bmatrix} \mathbf{\Delta P}(\mathbf{x}) \\ \mathbf{\Delta Q}(\mathbf{x}) \end{bmatrix} = \begin{bmatrix} P_1(\mathbf{x}) - P_1 \\ \vdots \\ P_{n-1}(\mathbf{x}) - P_{n-1} \\ Q_1(\mathbf{x}) - Q_1 \\ \vdots \\ Q_{n-1}(\mathbf{x}) - Q_{n-1} \end{bmatrix} = \mathbf{0} \tag{37}$$

5.1.2   Inequality: Technical Constraints

The operational constraints are the ones that ensure the system operates within the limits of the equipment. These constraints of inequality nature, setting upper and lower bounds for certain variables. They will be the inequality constraints $\mathbf{G}(\mathbf{x}) \leq 0$ in the optimization problem in Eq. 35. We will denote as $\mathbf{L_i^X}$ each different limit at bus i and for the sake of coherence we will express the constraints in the $\mathbf{G}(\mathbf{x}) \leq 0$ form.

Note that all the following limits can be based on grid code requirements, but we will use some standard values.

Bus voltage limits
We set the nodal bus-i voltage, V_i, limits as:

$$\begin{aligned} L_i^{Vu} = V_i - V_{max} \leq 0, \quad i \in N \quad &\text{is the upper limit} \\ L_i^{Vl} = V_{min} - V_i \leq 0, \quad i \in N \quad &\text{is the lower limit} \end{aligned} \tag{38}$$

where $\mathbf{V_{max}}$ and $\mathbf{V_{min}}$ are the maximum and minimum voltages. These values have been taken to be ± 0.1 p.u. of the nominal voltage respectively.

Maximum current limits for the lines
The current in the lines should not exceed the maximum current that the cables and transformers can handle. We will set $I_{max} = 1.1$ p.u. of the rated current of the cable I_{rated}. This rated current is given by manufacturers [4]. Therefore, the constraint will be:

$$L_i^I = I_i - I_{max} \leq 0, \quad i \in N_{lines} \tag{39}$$

ETSEIB

Reactive power delivered to the grid

In general reactive power delivered to the grid, Q_6 can be defined by grid code requirements. Nevertheless, in this work we will aim to keep it as close as possible to zero. Therefore, we will set the limits as:

$$L_6^{Qu} = Q_6 - Q_{max} \leq 0$$
$$L_6^{Ql} = Q_{min} - Q_6 \leq 0$$

$$(40)$$

where $Q_{max} = Q_{min} = 0$. Also note that potentially the wind turbines could be used to absorb reactive power, but we will not consider this option in our work.

5.2 Objective Function

Probably one of the critical parts is to identify the objective function we want to minimize and decide how we treat it. Now, we will describe the terms that we will include in the objective function and why we have decided to work with a multi-objective approach.

5.2.1 Why Bi-objective?

Let us imagine you are an engineer of a firm that is planning to build and OWPP. You have to ensure both that the transmission system is reliable and robust in terms of operational constraints but also to make the investment as profitable as possible, therefore you want to minimize its investment cost. Given this scenario, you can expect that it exists a trade off between the two objectives, investing more money can make your transmission system more robust and yield smaller power losses and vice versa. In fact, in eRoots project for Acciona, they have shown interest on getting insights on how these two objectives interact with them and decide which option to go for given the relationship.

Literature can offer solutions for this kind of scenarios. Multi-objective optimization, also known as Pareto optimization, deals with situations where optimal decision-making needs to be taken in presence of various conflicting objectives. Within this context, there is no guarantee that there exist a unique solution that minimizes both objectives. The main idea is to find the set of solutions that are not dominated by any other solution in the set; that is solutions where no objective can be further minimized without worsening another. In this sense, any point found in this set can be considered optimal and be regarded as a potential solution. This set is called the Pareto Frontier and the solutions are called Pareto optimal solutions.

Using the formulation in Eq. 35, let $\mathbf{x}^* \in \mathbf{X}$, where $\mathbf{X}$ is the feasible set of solutions that satisfy the constraints, have its associated outcome vector $\mathbf{f}(\mathbf{x}^*)$. Then a feasible solution $\mathbf{x_1}$ is said to (Pareto) dominate another solution $\mathbf{x_2}$ [14] if:

$$\forall i \in \{1, 2, ..., k\}, f_i(\mathbf{x_1}) \leq f_i(\mathbf{x_2}) \quad \text{(Condition 1)}$$
$$\exists i \in \{1, 2, ..., k\}, f_i(\mathbf{x_1}) < f_i(\mathbf{x_2}) \quad \text{(Condition 2)}$$

$$(41)$$

ETSEIB
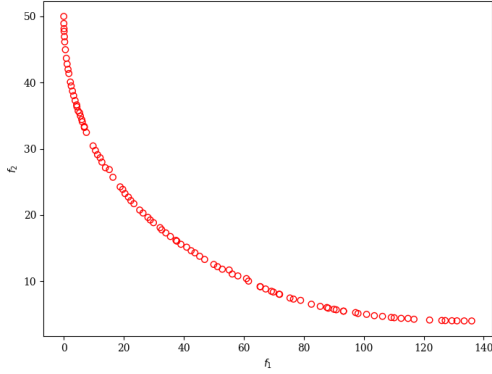
(a) Pareto Front for Binh and Korn function
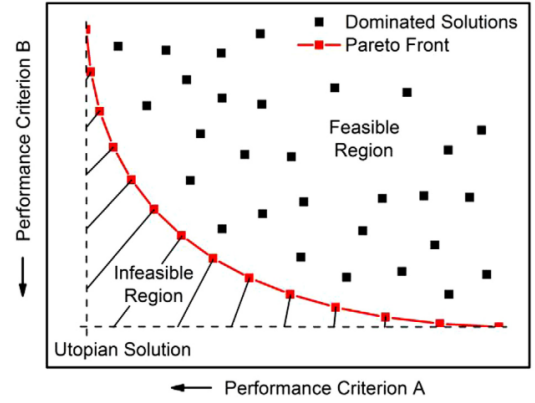
(b) Explanation of domination [18].

In Fig. 11a you can see the Pareto Front of the Binh and Korn function [17], a usual test function for multi-objective optimization.

Now we can go back to our problem and decide how to define both objectives. Therefore, we define the objective function as:

$$\mathbf{f}(\mathbf{x}) = (f_{invest}(\mathbf{x}), f_{tech}(\mathbf{x})) \tag{42}$$

where the definition of $f_{invest}(\mathbf{x})$ is quite straight-forward; the addition of the cost of the elements in the transmission system:

$$f_{invest}(\mathbf{x}) = C_{cables}(\mathbf{x}) + C_{tr}(\mathbf{x}) + C_{sh}(\mathbf{x}) + C_{gis-AC}(\mathbf{x}) + C_{ss-AC}(\mathbf{x}) \tag{43}$$

When it comes to how we handle $f_{tech}(\mathbf{x})$ it becomes a little more tricky. We wanted this part to capture how optimal is the transmission system, in terms of steady-state operational conditions and power losses. In other words, this term has to measure if the inequality constraints, the ones related to operational limits, are being satisfied and try to minimize $C_{loss_{AC}}$. To do so we will use a penalty method to deal with the inequality constraints.

Exhaustive development of this method can be found in [19], but the main idea is to expand the original feasible set of solutions, $\mathbf{X}$, to all of $\mathbb{R}^n$, but a large cost or "penalty" is added to the objective function when the solution is not satisfying $\mathbf{G}(\mathbf{x}) \leq 0$. Therefore:

$$f_{tech}(\mathbf{x}) = C_{loss-AC}(\mathbf{x}) + c \cdot \mathbf{p}(\mathbf{x}) \tag{44}$$

where c is the penalty factor and $\mathbf{p}(\mathbf{x})$ is the penalty function:

$$\mathbf{p}(\mathbf{x}) = \sum_{L_i^X \in G(x)} \max(0, \mathbf{L_i}(\mathbf{x})) \tag{45}$$

In practice, setting a big value for c will make the optimization method to look for solutions that satisfy the constraints.

5.3   Algorithm Overview

Now we have set up all the elements that define the sequential process for finding the desired Pareto Front. Now it just remains to find the recursive optimization method that that suits best our problem. Note that here we advance that we will use the genetic algorithm NSGA-II to solve the optimization problem (see section 6.2). Fig. 12 shows the block diagram of the solver implemented in Python (check the Appendix).
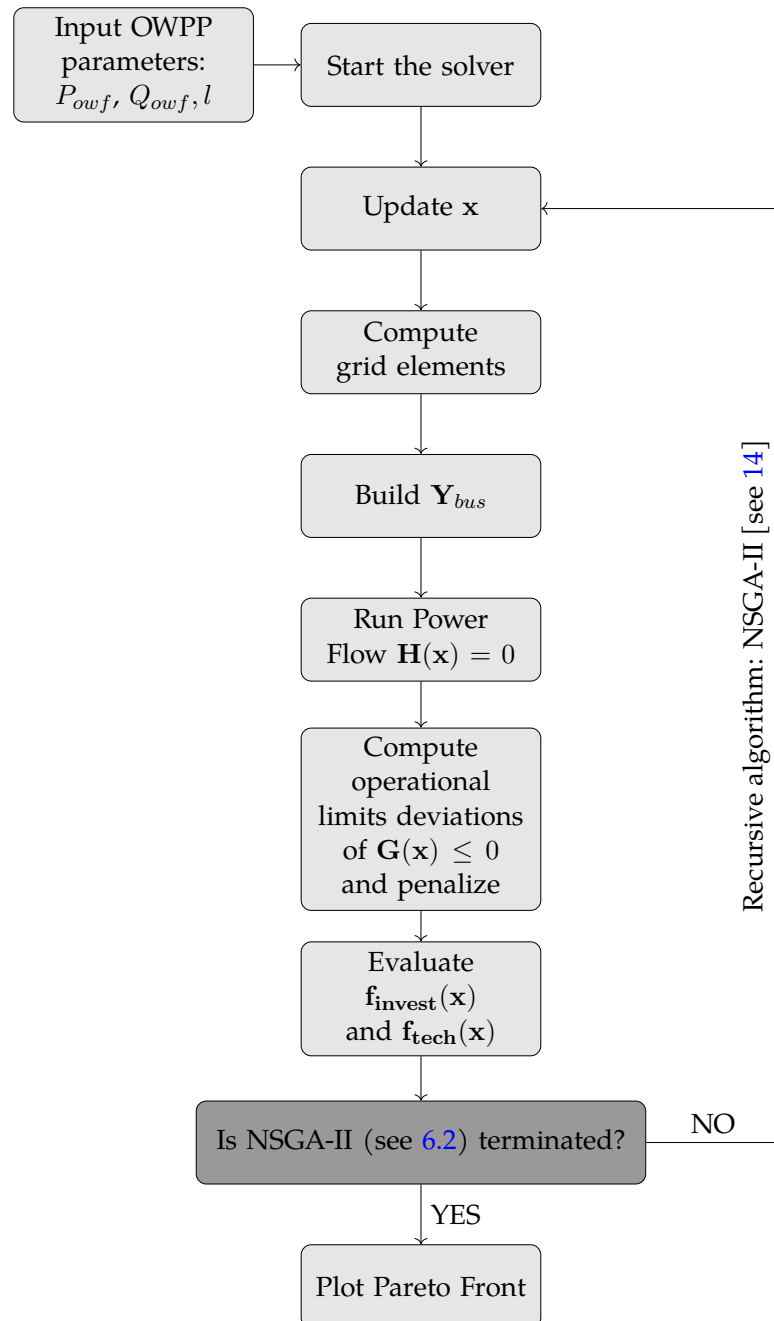
Figure 12: Block diagram of the optimization algorithm.

6 Optimization Methods

After what we have summarized in the previous section we want an optimization method that:

- Can handle mixed-variable optimization problems, meaning that it can handle binary, integer and continuous variables as decision vector **x**.

- Can handle bi-objective optimization problem with equality and inequality constraints and can deal with a penalty function.

- Can find the whole Pareto front to analyse the trade off between the two objectives, investment and technical.

6.1 State-of-the-art Limitations: Interior Point Method

In [1] they propose an iterative method for solving the reactive power compensation problem. This methodology solves the optimization for continuous variables using an interior point method solver [20] for every possible combination of integer variables. Then, they compare the total cost for all options and pick the one with smaller cost. The algorithm is summarized in Fig. 13:
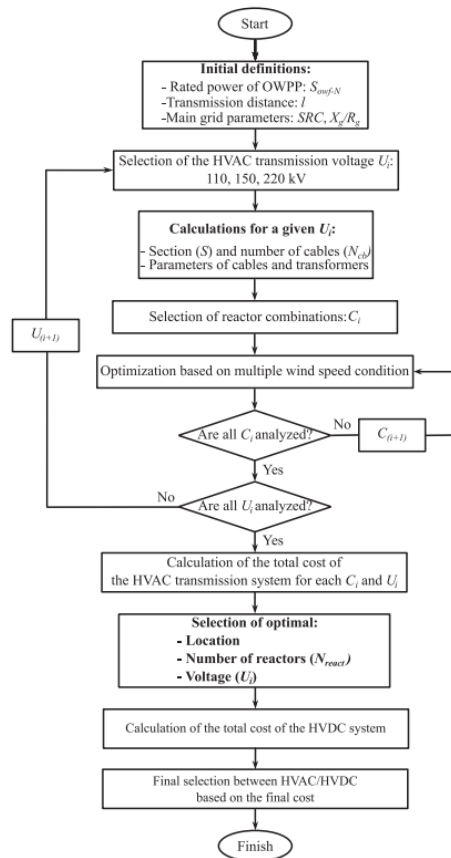

Figure 13: State-of-the-art algorithm for reactive power compensation optimization [1].

This method is not suitable for our case, as we want to find the whole Pareto Front and not just one optimal solution. Moreover, the number of possible combinations of integer variables can increase quickly in further expansions of the problem (for instance if you also consider the electrical collection system between turbines in the OWPP), making the method computationally expensive.

Another traditional method to solve multi-objective problems is to basically transform the problem into a single objective problem by using a weighted sum of the objectives [14]:

$$f(\mathbf{x}) = \sum_{i=1}^{k} w_i \cdot f_i(\mathbf{x}) \quad \text{where} \quad \mathbf{x} \in \mathbf{X} \text{ and } \sum_{i=1}^{k} w_i = 1 \tag{46}$$

From Eq. 46 is clear that modifying the weights w_i we change the relative importance we give to each objective. The main drawback of this approach, even though that we can deal with more than one objectives at the same time, we still get just one solution for each combination of weights, not a set of optimal solutions, i.e. the Pareto Front. Moreover, how do we choose this w_i? The optimal point is sensible to these weights, therefore you must have a clear understanding of you priorities between the objectives which is something we do not want to impose in our approach.

6.2   NSGA-II: Genetic Algorithm

This is where genetic algorithms (GA's) come into play. GA's are a class of optimization algorithms that are inspired by the process of natural selection that uses the principles of evolution to solve optimization problems. The main idea is that they start from a random population of candidate solutions and, in one single simulation run, they are able to find multiple Pareto optimal solutions.

That is why we will use the Nondominated Sorting GA II (NSGA-II) algorithm to solve our problem. It accomplishes the requirements in section 6. Moreover, it allows us to treat inequality constraints with penalty functions, as proposed in section 5.2.1.

An exhaustive theoretical development of how NSGA-II works is out of the scope of this work, but a complete and formal description of the algorithm can be found in [15]. Just for the sake of completeness, one can simplify how NSGA-II works in the recursive steps of Fig. 14:
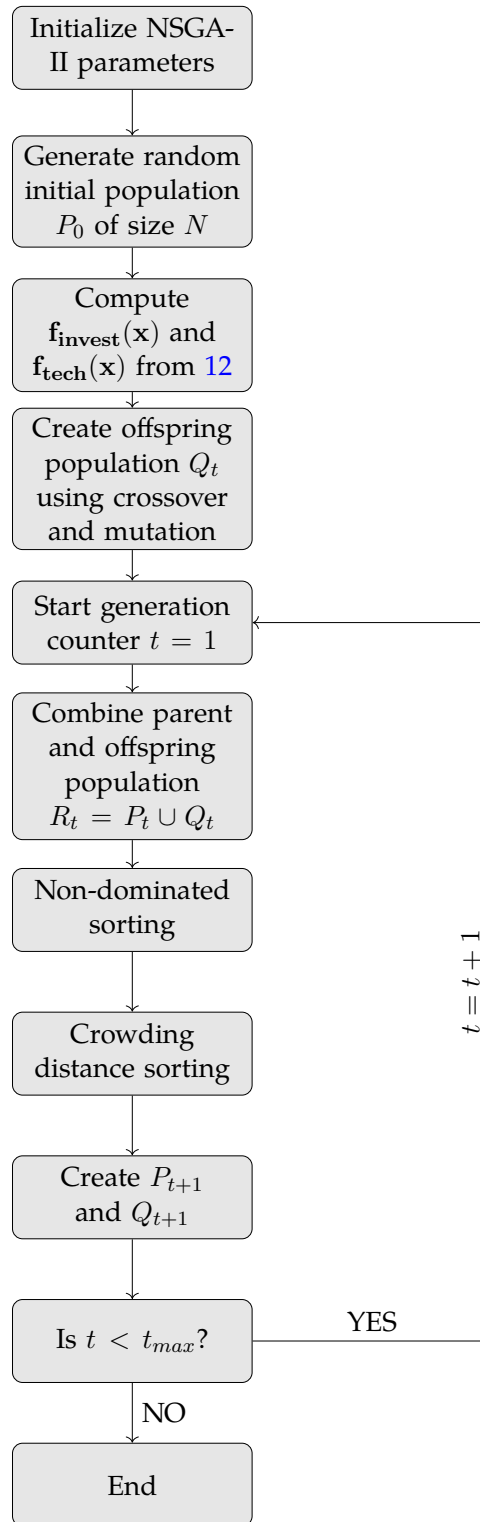
ETSEIB

Figure 14: Block diagram of NSGA-II

Regarding the description of the algorithm in Fig. 14:

1. Initially a random population P_0 of size N is created. This population is sorted according to

non-domination (which is an equivalent name for Pareto dominance) described in Eq. 41.

2. A new offspring population Q_t is created by applying crossover and mutation operators to the population P_t. Crossover combines two solutions $\mathbf{x}$'s to create a new one and mutations introduce small random changes, or mutations, to $\mathbf{x}$. This part is where the inspiration for the name of GA's comes from. Check [15] for further explanation.

3. The offspring population Q_t is combined with the parent population P_t to create a new population R_t of size $2N$. This population is sorted again according to non-domination.

4. Non-dominated sorting creates non-dominated sets F_i of solutions where i is the non domination level. The first set F_1 contains the non-dominated solutions, the second set F_2 contains the solutions that are dominated only by the solutions in F_1 and so on.

5. Crowding distance sorting basically creates the new P_{t+1} by selecting the best solutions in the non-dominated sets F_i until you arrive to size of N for the new population.

6. The algorithm iterates until the maximum number of generations t_{max} is reached, which will be the termination condition.
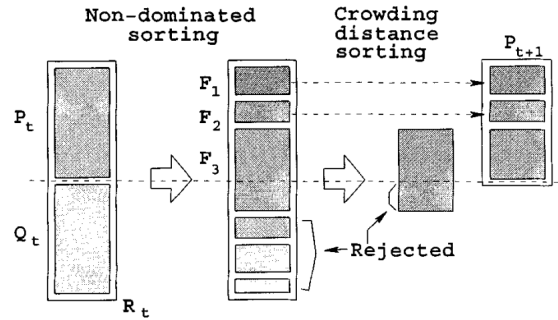

Figure 15: Visualization of steps 4 and 5 [15].

The algorithm in Fig. 12 has been implemented in pymoo [16], a Python library for multi-objective optimization that includes the NSGA-II algorithm 14 and allows formulating mixed-variable problems. It is worth mentioning that the proposed method in Fig. 12 is performed on a whole set of N candidate solutions $\mathbf{x}$ from the population set P.

6.3 Optimal Power Flow Approach for Compensation Optimal Sizing

In this section we propose a different approach based on the Optimal Power Flow (OPF) to validate the results obtained with NSGA-II, specifically the ones relates to the sizing of the reactive power compensation.

The idea is to take one optimal solution from NSGA-II, i.e. all the decision variables in $\mathbf{x}$, and recom-

pute just the values of sizing of the shunt reactors Y_{sh_i}. The main idea is to compare how close is the stochastic approach solutions of NSGA-II to the solutions given by a standard deterministic approach as the OPF.

The traditional AC-OPF objective function [21] minimizes de cost of generating active power:

$$\min_{P_G} \quad \mathbf{c^T P_G} \quad \text{where} \quad \mathbf{c} = \begin{bmatrix} c_0 \\ c_1 \\ c_2 \end{bmatrix} \tag{47}$$

where $\mathbf{P_G}$ is the vector of active power generated by the generators and c_0, c_1 and c_2 are the independent, linear and quadratic power generations costs respectively.

As we saw in Eq. 13, shunt reactors compensate a reactive power equivalent to $Q_{sh} = Y_{sh} \cdot U^2$. Therefore, finding the optimal size of the shunt reactors is equivalent to minimize the cost of the reactive power compensation. Therefore, we can modify the objective function of the OPF to:

$$\min_{Q_{sh}} \quad \mathbf{c_{sh}^T Q_{sh}} \quad \text{where} \quad \mathbf{c_{sh}} = \begin{bmatrix} K \\ P \\ 0 \end{bmatrix} \tag{48}$$

where K and P are from Table 4.

We have made this modifications implemented in the AC-OPF solver in GridCal [22], an open-source Python library for power systems analysis. Note that the derivatives of the objective functions, Jacobian and Hessian, have been modified according to the new objective function 48.

ETSEIB

7 Case Study

In this section we will study in depth the results that the algorithm yields for a specific design parameters of an OWPP. We will benchmark the results obtained with NSGA-II with a "brute" force approach using random search and compare the results of reactors sizing comparing with the OPF approach. Moreover, we will do an in-depth analysis of the optimal solution cost breakdown and compare it to optimal points without considering reactive power compensation to understand the need to include this in the optimization problem.

The results obtained have been computed in a laptop with the following specifications:

- Processor: Processor: Intel(R) Core(TM) i5-8365U CPU @ 1.60GHz

- RAM: 8 GB

- OS: Windows 11

- IDE: Visual Studio Code and PyCharm

- Python version: 3.11.8

- Pymoo version: 0.6.1

- GridCal version: 5.1.11

The tuning parameters used for initializing the NSGA-II algorithm are shown in Table 9.

Parameter	Value
Population size, N	150
Survival sorting	Rank and Crowding "pcd"
Termination, t_{max}	15 generations
constraint penalty, c	10e4

Table 9: Tuning parameters NSGA-II.

It is worth mentioning that NSGA-II has a time complexity of $\mathcal{O}(MN^2)$, where M is the number of objectives and N the population size. With $M = 2$ and setting $N = 150$ and $t_{max} = 15$, it takes the algorithm about 10 s to terminate. To put this performance in perspective, the method proposed in [1] and described in section 6.1 needs between 45 and 140 s to find the optimal solution.

7.1 500 MW, 100 km OWPP

We pick as case study a 500 MW OWPP located 100 km from shore. Results have been separated in different subsections to study specific results.

ETSEIB

7.1.1 Random Search compared to NSGA-II

In this section we compare the results obtained with NSGA-II with a brute force approach. This simply means that we generate a random population of solutions within certain bounds that guarantee power flow convergence on most of the cases and evaluate the objective function with those solutions. For the sake of a fair comparison, we showcase the results obtained with the two methods at the same computation time of around 10 s, which corresponds to 700 random evaluations.

In Fig. 16 we can see how both the NSGA-II and the random search are distributed in the objective function $\mathbf{f}(\mathbf{x})$ 2-D space. To give some intuition on what we see, each set of black points (random evaluations) is characterized by a dominant term in the investment cost value, normally the number of cables or the placing of a shunt reactor mid-cable both of which introduce big changes in the investment cost. The red points (NSGA-II) is the set of Pareto dominating solutions.
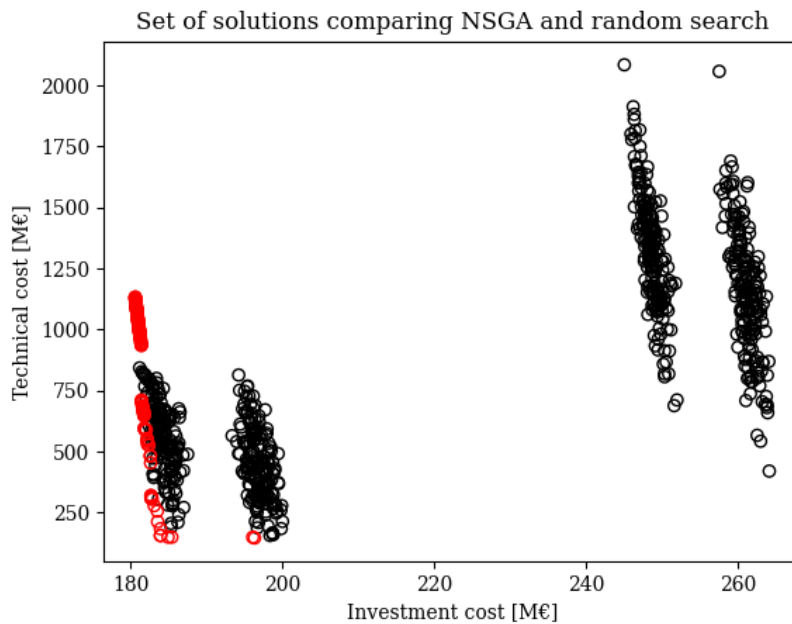

Figure 16: Random search (black) compared to NSGA-II (red).

From the results in Fig. 16 and the zoom on the Pareto area on Fig. 17 we can see that:

- NSGA-II is able to find the set of optimal solutions in the region closer to the utopia point, i.e. where both objectives are equal to 0.

- The Pareto front is well-defined and the solutions are well distributed.

- NSGA-II is able to find solutions that are non-dominated by the random search. This means that the algorithm effectively outperforms any kind of brute force approach since it reveals a set of solutions F_1 that dominates all the random search points.
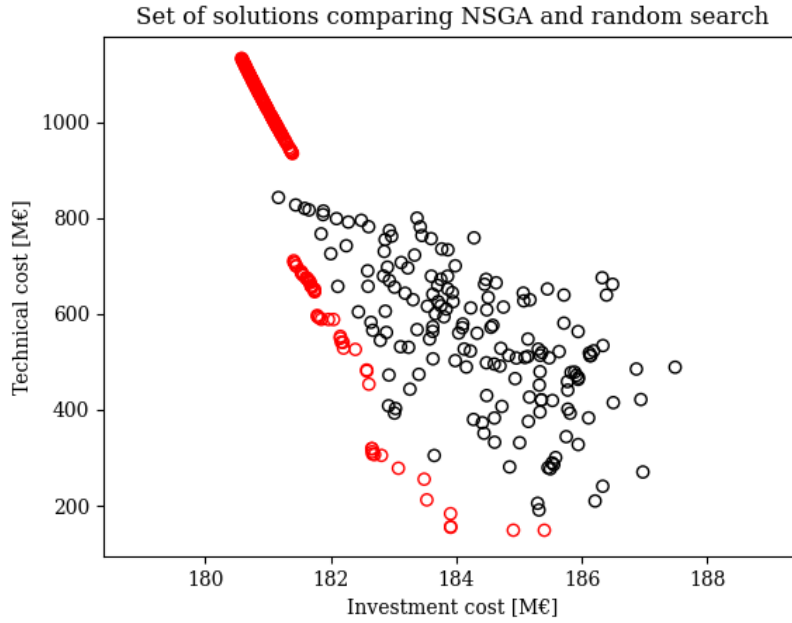
Figure 17: Zoom on the Pareto Front area, random search (black) compared to NSGA-II (red).

Note in Fig. 17 we see a weird behaviour on the upper-left side of the Pareto front. It seems that in that region, the one corresponding to not including any shunt reactor, there are some random search points that dominate the NSGA-II results. This should not be the case and our hypothesis is that it is related to the random sampling of binary variables (the one corresponding to the locations of the shunt reactors) of the initial population P_0 and how is unable to generate a well-distributed population of candidate solutions. Future work should focus on how to improve the initial population sampling of all types of variables and hopefully solve this issue.

7.1.2   OPF Validation

Now we showcase how the OPF approach helps to validate the results obtained with NSGA-II. We pick one point from the Pareto Set and take its solution for all the variables in **x** except for the continuous variables of the sizing of the reactors, Y_{sh_i}.

We will use a random point of the non-dominated set, arbitrarily chosen to be the one minimizing both objectives with equal weights. This essentially is converting the multi-objective problem into a single objective one using the method proposed in section 6.1 with $w_{invest} = w_{tech} = 0.5$. The optimal solution we get from NSGA-II is presented in Table 10:

Parameter	Value
Transmission voltage level	220 kV
Number of cables	2
Reactors	$[1, 1, 0, 1, 0]$
Rated power of the transformer	509.72 MVA

Table 10: Specifications (excluding reactors sizing) of the optimal solution.

Now, we run the OPF proposed in Eq. 48 and implemented in GridCal and compare the results. Initially, we check the convergence and running time of the OPF:
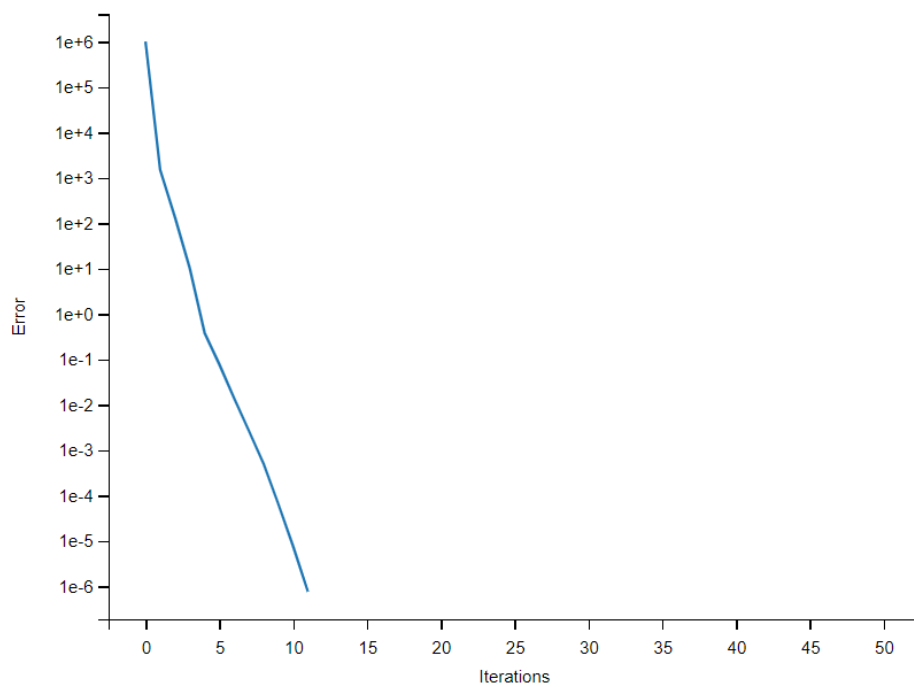

Figure 18: OPF convergence

Fig. 18 shows how the OPF converges to the optimal solution in 12 iterations, and it takes about 1.5 seconds. For comparison, running the traditional PF in 4.6.2 takes around 0.06 s. That makes OPF around 25 times slower than the traditional PF.

Afterwards, we check the values Y_{sh} obtained from the OPF and see how they affect the objective function:
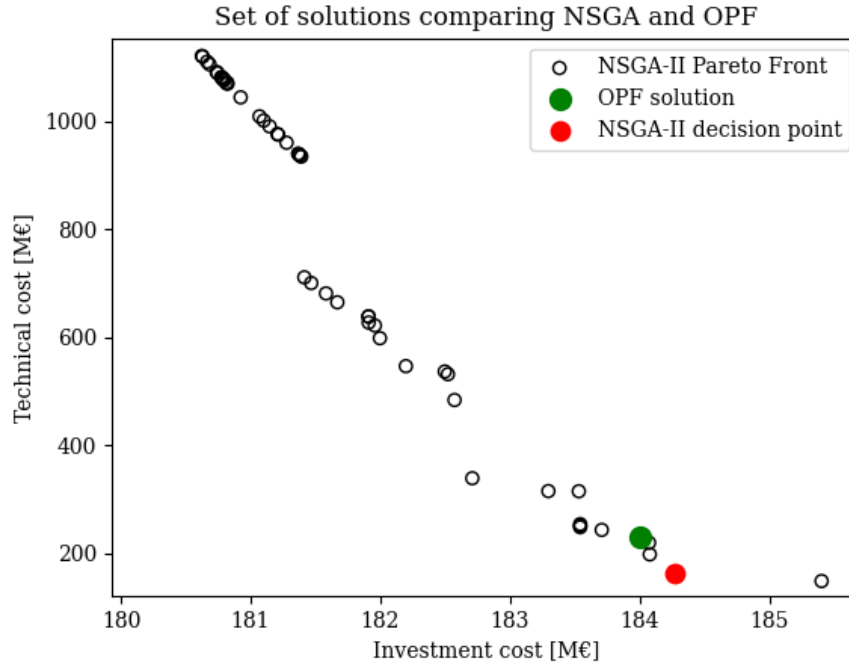
Figure 19: NSGA-II vs OPF for reactors sizing.

As we see in Fig. 19, the OPF gives a solution that is very close to the one obtained with NSGA-II and most importantly, the OPF solution does not dominate the NSGA-II solution. The fact that the point is not exactly the same is because OPF and NSGA-II penalization costs are defined differently and cannot be compared directly. Nevertheless, the important property is that both solutions fall in the same Pareto front.

This validates the results obtained with NSGA-II since OPF, which is a strictly traditional optimization method, does fall on the same non-dominated set F_1, meaning that it has not found a combination of reactors sizing that Pareto dominates the solutions from NSGA-II.

7.1.3 Costs Break Down

In this section we will break down the investment costs terms of the optimal solution presented in Table 10 and compare it to the same solution eliminating the reactive power compensation given by the shunt reactors. The idea is to quantify to effect of reactive power compensation in the power losses of the transmission system and the need to include it in the optimization problem. The results are presented in Fig. 20 and Fig. 21:
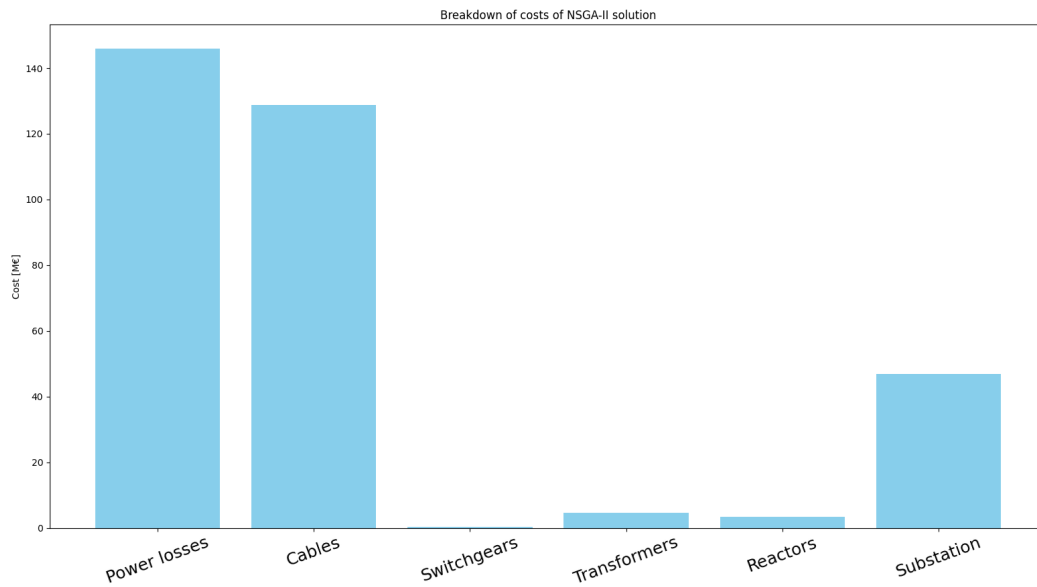
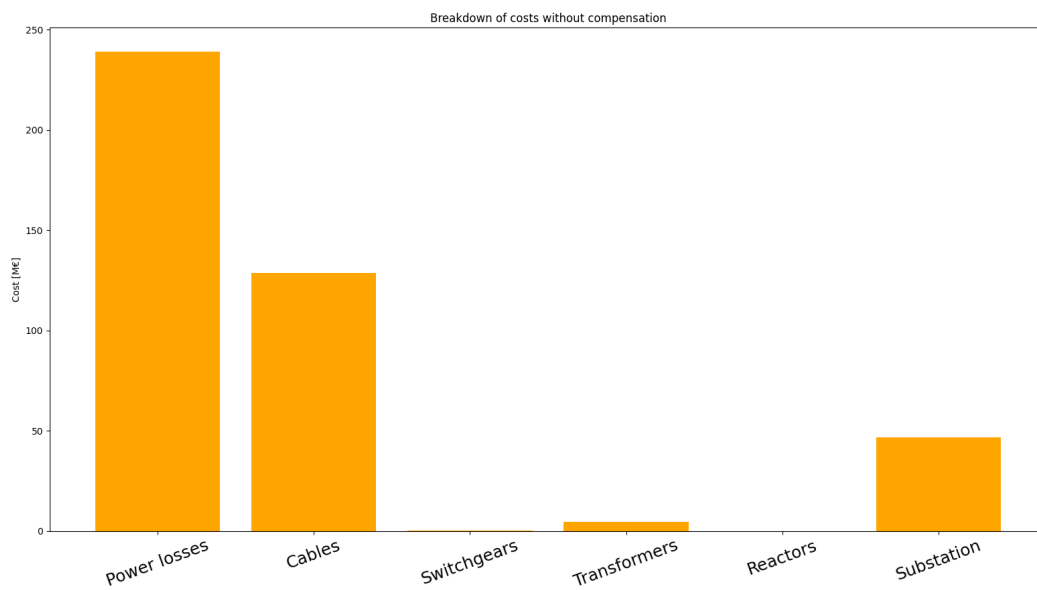Figure 20: NSGA-II optimal solution cost break down.

Figure 21: No compensation solution cost break down.

Note the different scales in the y-axis of Fig. 20 and Fig. 21 and how power losses, cables and substation cost are the dominant ones. For the sake of clarity we can compare both cumulative total costs in the same plot as seen in Fig. 22:
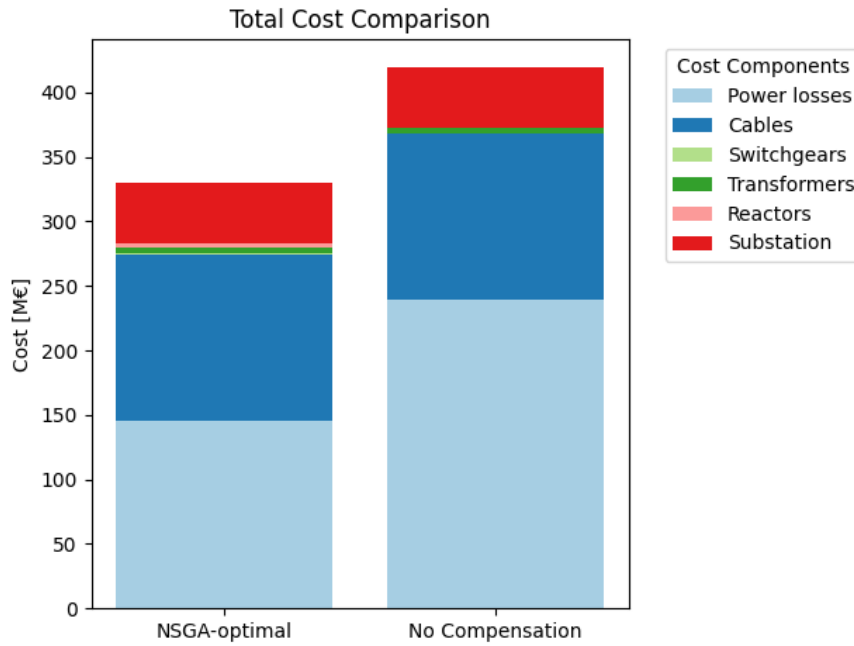
Figure 22: NSGA-II optimal solution and no-compensation total cost comparison.

The main conclusions we can extract from the results in Fig. 22 is that the cost of including shunt reactors is very profitable since an extra $3.35M€$ in investment cost is translated into a $93.2M€$ reduction in the power losses costs, an impressive 39% reduction.

From this section the need of reactive power compensation is clear. Moreover, future work presented in the next section 7.1.4 and in section 8.2 will showcase how this compensation becomes even more important when we consider a variable power injection from the OWPP.

7.1.4 Power Losses and Overvoltage with Variable Power Injection

This section will serve as a breeding ground for future work, check 8.2. We want to see how the power losses and overvoltages evolve with power injections below the nominal value using the optimal solution we have found considering that $P_{owf} = 500$ MW always. Also, we will check what happens if we eliminate the reactive power compensation to compare how effective is to include these shunt reactors in the optimization problem. The results are presented in Fig. 23 and Fig. 24:
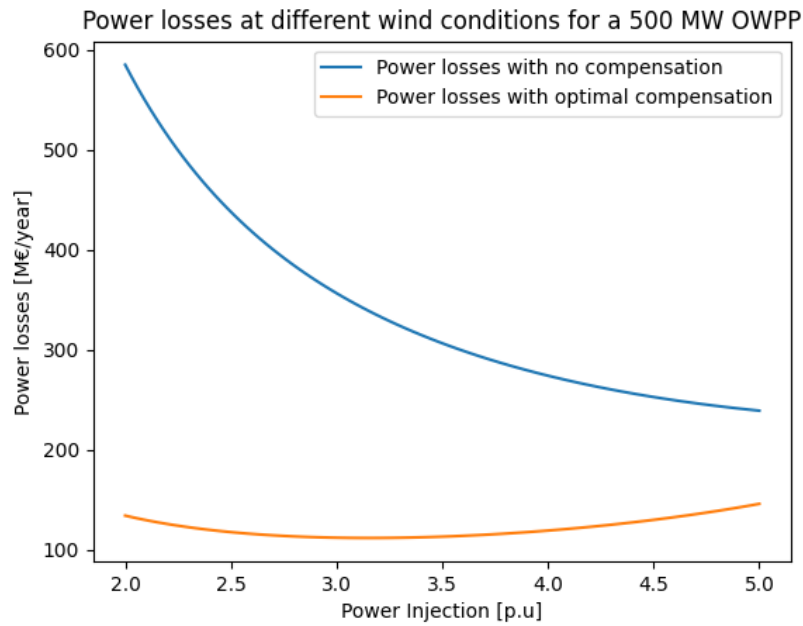
ETSEIB

Power losses at different wind conditions for a 500 MW OWPP

Figure 23: Power losses evolution with variable power injection.

From Fig. 23 we see how the power losses increase exponentially as we reduce P_{owf} when no reactive power compensation is considered. This is due to the fact that the power losses are directly proportional to the square of the current in the transmission lines and the reactive power compensation helps to reduce it when p_{owf} decreases. As to the optimal compensation solution we observe that power losses (as expected from 1) are kept relatively low for all power injections considered, showcasing how useful shunt reactors are for limiting power losses in presence of variability of the power injection.
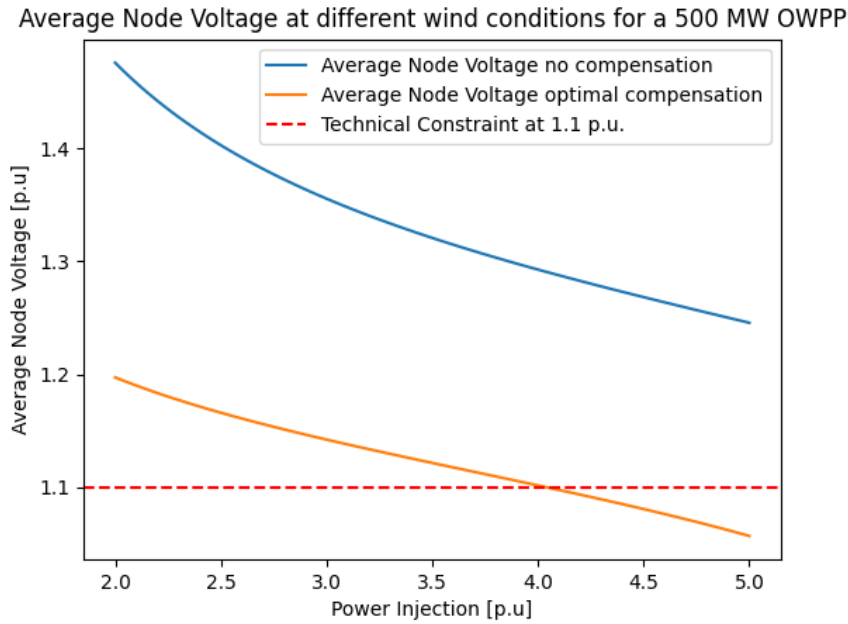
Figure 24: Overvoltage evolution with variable power injection.

From Fig. 24 we see that reducing the power injection also increases V_{avg}, which is the average of all nodes in the transmission system voltage level in p.u. Again, shunt reactors effectively manage to keep V_{avg} below the limit of 1.1 p.u. (which no compensation cannot do) but up to a certain point where the power injection is so low that the shunt reactors are not able to compensate the reactive power enough to keep the voltage level below the technical limit. It is clear from the optimization in Eq. 35 that if we want to satisfy operational limits, we need to increase the reactive power compensation in the optimal solution if lower P_{owf} are considered.

Considering a distribution for the wind speed, as proposed in section 8.2, will include this distribution of power injections below the nominal value and will give a more realistic view of the system and the need for reactive power compensation.

ETSEIB

8 Conclusions

All the objectives proposed at the beginning in section 2.3 have been accomplished. This chapter summarizes the main conclusions of the work and presents some proposals to take into consideration for future related work.

8.1 Outcome

The main outcomes derived from the objectives met from each chapter of interest are:

- Chapter 5 covers the mathematical fundamentals of the problem formulation and optimization approach. The analysis shows how the multi-objective approach helps us achieve the desire to obtain the full Pareto Front and how this approximation becomes useful to understand the underlying behaviour of the power flow analysis of the transmission system model.

- Chapter 6 presents the state-of-the-art optimization algorithm and presents the different techniques that have been considered to be used. It establishes the limitations that have been found and how the applications of a genetic algorithm such as NSGA-II can help to overcome them and meet the requirements of the optimization problem. It presents some theoretical fundamentals of the algorithm used and the schematic of the recursive solver that has been implemented.

- Chapter 7 applies the optimization algorithm to a specific case study of an OWPP. First, the algorithm implementation has been demonstrated to be fully functional and meets the requirements in section 6. The results show how we obtain a coherent Pareto Front and how the results obtained outperform any brute force approach, revealing a set on non-dominated optimal solutions. Moreover, the comparison with the OPF approach validates our results and shows that NSGA-II is able to reach the "best" points using a stochastic approach given that OPF is unable to explore any dominating area below the Pareto Front. The cost breakdown and evolution of cots for different power injections give an intuitive explanation of the need for reactive power compensation.

  All in all, it can be concluded that the innovative approach of using a GA for the optimization of the transmission system of an OWPP has been successful, and it has promising properties as a potential powerful tool to deal with this kind of optimization with reduced computational time.

8.2 Future Work

The implementation of NSGA-II for the optimization of OWPP transmission system design has potential to become a powerful tool. In this section we will propose a set of possible improvements that could enhance the overall quality of the proposed method and give new insights.

The main simplification and assumption through the development of the work has been assuming a constant power supplied by the OWPP at its nominal value, in other words, we are assuming a

constant wind speed at the desired value. As shown in Fig. 1 and in section 7.1.4, the need of reactive power compensation increases as the power injections of our plant decreases, i.e. low wind or no wind. The next and logical step is to let the proposed algorithm to consider different wind conditions. To be more accurate, we should consider a wind speed distribution, normally assumed to follow a Weibull distribution shown in Fig. 25.
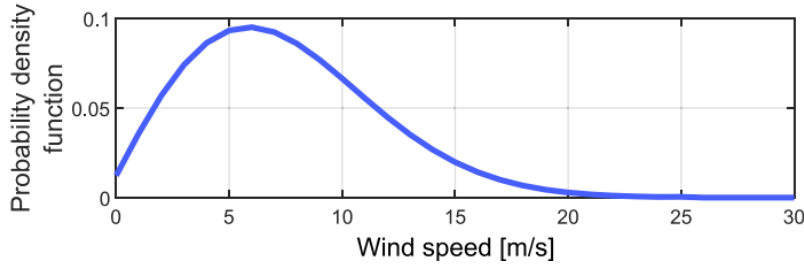

Figure 25: Weibull's distribution of wind speeds [1].

To consider this distribution, we propose to create a set of N wind speeds u_j, and associate a probability p_j and power generation P_{owf_j} to each of them. Now it would just remain that the step on which we solve the power flow in Fig. 12 to compute a weighted average of the power injections of the OWPP, P_{owf} with the probabilities p_j. Doing so, the objective function will be a weighted sum of the costs of the different wind conditions:

$$
\begin{aligned}
f_{invest}(\mathbf{x}) &= \sum_{j=1}^{N} p_j \cdot \left[C_{cables}(\mathbf{x}) + C_{tr}(\mathbf{x}) + C_{sh}(\mathbf{x}) + C_{gis-AC}(\mathbf{x}) + C_{ss-AC}(\mathbf{x}) \right] \\
f_{tech}(\mathbf{x}) &= \sum_{j=1}^{N} p_j \left[\cdot C_{loss-AC}(\mathbf{x}) + c \cdot \mathbf{p}(\mathbf{x}) \right]
\end{aligned}
\tag{49}
$$

This approach will give a more realistic view of the system and allow to do a fair comparison between the state-of-the-art results in terms of reactive power compensation sizing for every different combination of P_owf and l for OWPP.

Moreover, recall that we have limited our work to the HVAC technology, but HVDC technology should also be considered as an option. Literature [1] shows that after considering shunt reactors for reactive power compensation purposes, after the break-even distance of around 150 km, using HVDC becomes cheaper than HVAC, for which power losses increase notably for high distances. Computing costs for HVDC would allow to extend the decision variables of the optimization to its full domain of possibilities.

Moreover, further work could be to consider how disturbances of the voltage of the grid we are supplying to or the layout of the electrical collection system (see Fig. 26) inside the OWPP could affect the optimization problem. Also, this work could be implemented in a software like GridCal. Implement-

ing this algorithm in an open-source software would allow to make it accessible to a wider audience, with a more user oriented interface and to be used in real-life projects.
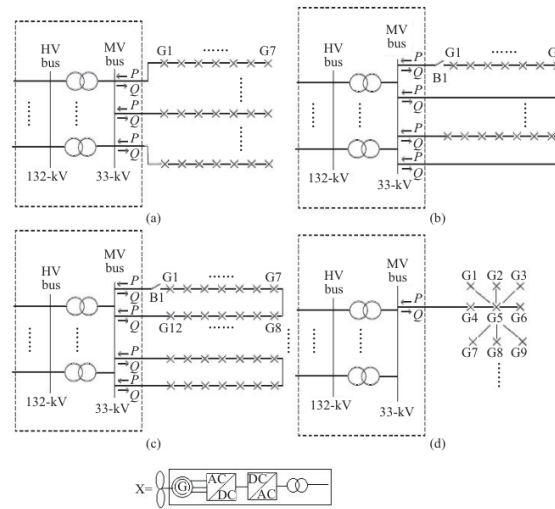

Figure 26: Collection system for some OWPP possible layouts: Radial(a), Single-sided ring(b), Double sided ring(c) and star(d) [24].

Finally, one of the main criticism to this work would be the validity of the cost functions used for the objective function. Finding and approximating this functions is no easy work, since costs associated to each element vary from manufacturer to manufacturer and cost analysis can be extended not just initial investment ones, but to other concepts such as maintenance, operation and depreciation costs. Studying more complex and accurate versions of costs functions is another potential line of work.

All in all, the work developed in this thesis provides a good theoretical and practical basis for further research in the optimization of transmission systems in OWPP. In fact, this thesis will be used as the starting point for eRoots and Acciona to implement an operative and complete version of the algorithm in GridCal.

9 Planning and Viability Studies

9.1 Time Planning

Fig. 27 shows the time distribution for the tasks carried out in the thesis.
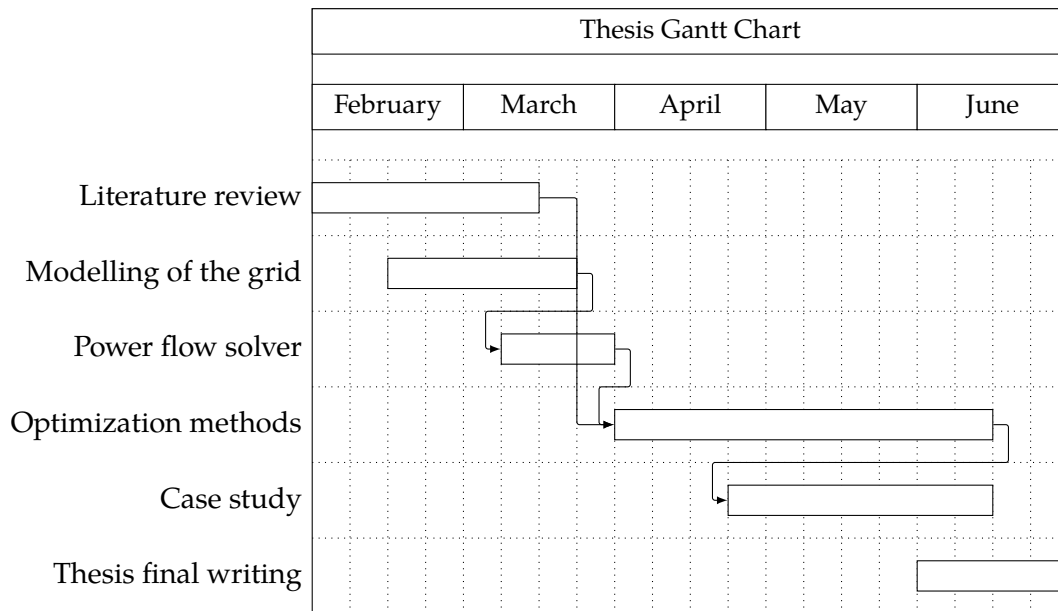

Figure 27: Thesis Gantt Chart.

9.2 Economic Assessment

The budgeting for this work includes the human resources used during the development of the thesis. We have considered the working hours devoted to the project under the internship agreement, as well as an average of 2.5 hours per week of tutor supervision. The total cost has been broken down with and without the Value Added Tax (VAT). The complete budgeting is shown in Table 11.

Concept	Unit Cost	Quantity	Total (€)
Working hours	8 €/h	450 h	3600
Tutor supervision	25 €/h	50 h	1250
Total without VAT			4850
Total with VAT (21%)			5868.5

Table 11: Thesis Costs.

Note that the computer used for the development of the thesis has not been included in the budgeting, as it was already owned by the author and well-beyond its amortization period.

ETSEIB

9.3   Environmental Assessment

9.3.1   Energy Consumption

This environmental assessment evaluates the energy consumption costs incurred during the development of a thesis over five months, using a computer as the primary tool. The primary energy consumption arises from the computer's usage, which includes writing, research, data analysis, and communication.

Assuming an average laptop with a power consumption of 60 watts, used for approximately 6 hours daily, the total energy consumption over five months is around 54 kWh. This consumption translates to roughly 30 kg of CO_2 emissions, assuming the average emission factor for electricity generation.

To reduce these energy costs and associated environmental impacts in future thesis projects, several strategies can be employed. Utilizing energy-efficient computers, enabling power-saving modes, and limiting usage time can significantly lower consumption. Additionally, adopting renewable energy sources, such as solar panels for charging devices, further reduces the carbon footprint, contributing to a more sustainable academic practice.

9.3.2   Potential Impact

Optimizing transmission systems in OWPP can significantly enhance environmental impact by maximizing energy efficiency and reducing carbon emissions. Improved transmission reduces energy losses, ensuring that more clean energy reaches the grid, thereby displacing fossil fuel-based power generation. Additionally, optimization can lead to less intrusive infrastructure, minimizing harm to marine ecosystems and reducing the physical footprint of OWPP. Efficient transmission systems also facilitate the integration of larger amounts of renewable energy, supporting the transition to a sustainable energy future and helping to combat climate change by lowering greenhouse gas emissions.

9.4   Social and Gender Equality Assessment

This assessment evaluates the social and gender equality aspects of a bachelor's thesis focused on developing a tool for optimizing renewable energy system design, authored by a 22-year-old white engineering student. While the thesis itself addresses a critical area in sustainable development, examining its social dimensions is essential to ensure inclusivity and equality.

The demographic profile of the author reflects broader trends in STEM fields, where women and minority groups remain underrepresented. This lack of diversity can influence the perspectives and priorities embedded in the research. Ensuring diverse representation in such projects is crucial for incorporating a wide range of insights and addressing the needs of various communities.

To promote social and gender equality, the research should consider the differential impacts of renewable energy systems on diverse populations. This approach ensures that the developed tools and

ETSEIB

technologies are accessible and beneficial to all segments of society.

Moreover, educational institutions should encourage and support participation from diverse backgrounds in engineering and renewable energy fields. Mentorship programs, scholarships, and targeted recruitment can help bridge the gender and social gap, fostering an environment where innovative solutions for renewable energy are developed through diverse and inclusive contributions.

Acknowledgements

Primer de tot vull agraïr profundament el suport constant del Josep, el meu tutor, que m'ha donat consell i ajuda quan l'he necessitada cada dia des de que vaig entrar a eRoots. Per extensió, agraïr la rebuda i suport de tot l'equip d'eRoots durant aquests mesos, especialment al meu tutor acadèmic, l'Oriol, que ha proporcionat noves idees i enfocs al desenvolupament del treball.

Aquest TFG tanca un capítol de quatre anys de la meva vida que han sigut molt feliços gràcies als meus amics del grau; gràcies a tots nou.

Finalment, agraïr a la meva família i a la Mire el seu suport incondicional cada dia i a ensenyar-me a estimar.

ETSEIB

Bibliography

[1] J. Dakic, M. Cheah-Mane, O. Gomis-Bellmunt, and E. Prieto-Araujo, *"HVAC Transmission System for Offshore Wind Power Plants Including Mid-cable Reactive Power Compensation: Optimal Design and Comparison to VSC-HVDC transmission"*, IEEE Trans. Power Del., vol. 36, no. 5, pp. 2814–2824, Oct. 2021.

[2] *Global Sustainable Development Report (GSDR) 2023*, United Nations, 2023. [Online]. Available: Global Sustainable Development Report (GSDR) 2023

[3] Orsted, *"Hornsea project"*, Orsted, 2024. [Online]. Available: Hornsea Project Three

[4] ABB High Voltage Cable Unit, *"XLPE Submarine Cable Systems: Attachment to XLPE Land Cable Systems - User guide"*, ABB, Karlskrona, Sweden, 2010.

[5] S. Jermouni et al., *"Overhead line Methodology: A methodology to desgin an overhead line"*, Rated-Power, September 2022.

[6] W. Wiechowski and P. B. Eriksen, *"Selected studies on offshore wind farm cable connections - challenges and experience of the Danish TSO"*, Proc. IEEE Power Energy Soc. General Meet.: Convers. Del. Elect. Energy the 21st Century, PES, 2008, pp. 1–8.

[7] ABB High Voltage Cable Unit, *"XLPE Cable Systems: User guide"*, ABB, Karlskrona, Sweden, 2010.

[8] Arthur R. Bergen, Vijay Vittal, *"Power systems analysis"*, 2nd ed. Tom Robbins, 2000.

[9] Kenneth Nazimek, *"Sparcity and decoupling in load flow analysis"*, New Jersey Insitute of Technology, 1977.

[10] Raquel García-Blanco *"Efficient solvers for power flow equations: parametric solutions with accuracy control assessment"*, Doctoral thesis, UPC, 2016.

[11] Goran Andersson, *"Modelling and Analysis of Electric Power Systems"*, ETH - Power Systems Laboratory, 2008.

[12] Stefan Lundberg, *"Performance comparision of wind park configurations"*, Chalmers University of Technology, 2003.

[13] Regional Group North Sea, *"Offshore transmission technology"*, ENTSOE AISBL, Brussels, Belgium, Tech. Rep., Nov. 2011.

[14] Kalyanmoy Deb, N. Srinivas, *"Multiobjective Optimization Using Nondominated Sorting in Genetic Algorithms*, Evolutionary Computation, Vol.2, Iss.3, September 1994.

[15] Kalyanmoy Deb, Amrit Pratap, Sameer Agarwal, T. Meyarivan, *"A Fast Elitist Non-Dominated Sorting Genetic Algorithm for Multi-Objective Optimization: NSGA-II"*, IEEE Transactions on Evolutionary Computation, Vol. 6, No. 2, April 2002.

[16] J. Blank, K. Deb, *"pymoo: Multi-Objective Optimization in Python"*,IEEE Access, vol.8, pp. 89497–89509, 2020. doi:10.1109/ACCESS.2020.2990567

[17] T. Binh, U. Korn, *"MOBES: A Multiobjective Evolution Strategy for Constrained Optimization Problems"*, Proceedings of the Third International Conference on Genetic Algorithms, pp. 176–182, Czech Republic, 1997

[18] Artur M. Schweidtmann et al. *Machine learning meets continuous flow chemistry: Automated optimization towards the Pareto front of multiple objectives"*, Chemical Engineering Journal, Vol. 352, Pg. 277-282, , 15 November 2018.

[19] Robert M. Freund *"Penalty and Barrier Methods for Constrained Optimization"* Massachusetts Institute of Technology, 2004.

[20] Richard H. Byrd, Jorge Nocedal, Charles Gilbert *"A Trust Region Method Based on Interior Point Techniques for Nonlinear Programming"*, Mathematical Programming, Vol. 89, Iss. 2, Pg. 149-185, 2000.

[21] S. Chatzivasileiadis *"Optimization in Modern Power Systems"*, Lecture Notes, Technical University of Denmark (DTU), September 2018

[22] S. Peñate *"GridCal: A Python Library for Power System Analysis"*, GitHub repository, 2021. [Online]. Available: , 2019

[23] L. P. Lazaridis *"Economic comparison of HVAC and HVDC solutions for large offshore wind farms under special consideration of reliability"*, Master thesis, KTH Royal Institute of Technology, 2015.

[24] P. Lakshmanan, R. Sun, J. Liang *"Electrical Collection Systems for Offshore Wind Farms: A Review"* CSEE Journal Of Power and Energy Systems, Vol.7, No.5, September 2021

Appendix

In the following link you can find the Git repository with all the code used for the development of this work: https://github.com/Ch4rlieStone/tfg_eroots